Bootleg Fire: evaluating the role of fuel treatments in mitigating burn severity near Sycan Marsh, Oregon

Astrid Sanna

A thesis

submitted in partial fulfillment of the

requirements for the degree of

Master of Science

University of Washington

2024

Committee:

Van R. Kane

L. Monika Moskal

C. Alina Cansler

Program Authorized to Offer Degree:

School of Environmental and Forest Sciences

University of Washington

Abstract

Bootleg Fire: evaluating the role of fuel treatments in mitigating burn severity near Sycan Marsh, Oregon

Astrid Sanna

Chair of the Supervisory Committee:
Van R. Kane
School of Environmental and Forest Sciences

Wildfires in western US dry forest ecosystems have increased in frequency and severity during recent decades due to a warming climate and a century of fire suppression. The 2021 Bootleg Fire in south-central Oregon provided a great opportunity to evaluate fuel treatment effectiveness near the Sycan Marsh Preserve, where pre-fire LiDAR data were also available. Within this study area, The Nature Conservancy (TNC), The Klamath Tribes (TKT), and the USDA Forest Service conducted mechanical thinning (Tx), prescribed fire (Rx), and both treatments combined (TxRx), through a collaborative partnership, over 16 years preceding the wildfire. We conducted a burn severity assessment one year after the Bootleg Fire, accounting for the local variability of top drivers, fuel treatments, and firefighting operations. We modeled the influence of burn severity drivers using Random Forests and examined their influence at a global and local scale using SHapley Additive exPlanations (SHAP) analysis.

In units treated with Rx and TxRx, the percentage of area burned at low severity was 86% and 83%, respectively; for both treatments, moderate and high burn severity accounted for

less than 15% and 5% of the area burned. In contrast, in units treated with Tx, the percentage of area burned at low, moderate, and high severity was 30%, 45%, and 25%, respectively. Finally, in untreated forests, the percentage of area burned at low, moderate, and high severity was 31%, 27%, and 42%, respectively. Top predictors included Rx, evaporative stress Index, 4km-window topographic position index, and canopy cover, in descending order of importance. Predictors related to firefighting operations and Tx were ranked third-to-last and last, respectively. Where fire suppression occurred, we observed a decreasing trend in predicted burn severity within units treated with Rx and more variable effects within Tx units. The local effect of each predictor varied spatially.

Our results and the testimonials of local managers indicate that fuel treatments involving prescribed fire were the most effective at mitigating burn severity and facilitated firefighting operations. Top drivers that initially seemed to reflect water-stress conditions and topographic positioning turned out to be proxies for fuel structure and accumulation, further underscoring the key role of fuel characteristics in affecting burn severity. These methods allowed us to interpret relationships that would have otherwise been overlooked or potentially misunderstood in an exclusively global analysis, rather than one that considers both global and local perspectives.

This study contributes to the body of knowledge by providing a reproducible framework to explain the effect of contagious processes like fire at both global and local scales. Additionally, it provides valuable lessons to guide and improve fire and fuel management practices across multi-ownership landscapes.

TABLE OF CONTENTS

LIST OF FIGURES

LIST OF TABLES

Acknowledgments

Special thanks to all the collaborators at The Nature Conservancy, especially Craig Bienz, Katie Sauerbrey, and Ryan Haugo, for generously sharing their knowledge of my study area and providing support throughout my master's program. Thank you to my committee members, Van Kane, Alina Cansler, and Monika Moskal, for providing me with indispensable assistance and advice. I'm grateful to Susan Prichard and Andrew Hudak for serving as committee members and providing great feedback and consistent encouragement. I'm also grateful to Caden Chamberlain, Nicholas Povak, and Liz van Wagtendonk for the inspiring conversations and constructive feedback on this project. I thank Alexander Howe for the invaluable coding advice. Many thanks to my lab mates for their good advice and the laughs we shared together. Most importantly, I wish to express my gratitude to Massimiliano, who has always believed in me and stood by my side, and to Elfrida for her most sincere friendship.

Lastly, I wish to acknowledge my dedication and resilience throughout this journey. I am grateful to myself for the hard work put into earning my master's degree and conducting this research, and for persisting through challenges.

This research has been supported and funded by The Nature Conservancy and carried out at the UW Forest Resilience Laboratory (FRL) and the Remote Sensing and Geospatial Analysis Laboratory (RSGAL).

Introduction

In historically fuel-limited dry forest ecosystems of western North America, continuous accumulation of biomass resulting from fire suppression combined with a rapidly warming climate has led to uncharacteristically large and severe wildfires (Allen et al. 2002; Van Mantgem et al. 2013; Halofsky et al. 2020; Hanan et al. 2021; Parks et al. 2023). Forests of the interior western US and Canada share a history of fire suppression, logging, gold mining, grazing, and the exclusion of Indigenous fire by Euro-American settlers since 1850 (Hessburg et al. 2019), which have significantly altered historical fire regimes (Wallace Covington 2000; Fry and Stephens 2006; Haugo et al. 2019; Hagmann et al. 2021).

Paradoxically, by becoming more effective at controlling and extinguishing wildfire, firefighting has created a condition of fire deficit (Parks et al. 2015b; Vaillant and Reinhardt 2017), and intensified the degrading effect of wildfires in fire-suppressed forests (Hagmann et al. 2022). For example, from 1984 to 2015, the forested area in Washington and Oregon that burned amounted to just one-tenth of what would have been expected under historical fire regimes (Haugo et al. 2019). The general fire deficit resulting from fire suppression finds its roots in a fire policy that was instituted to prevent catastrophic wildfires. In 1935, due to the Peshtigo Fire of 1871 and the three-million-acre Big Blowup of 1910, the US Forest Service instituted a policy of total fire suppression, aiming to eliminate fire from the landscape. Decades later, fire was recognized as an ecologically needed process that would benefit fire-prone ecosystems (Van Wagtendonk 2007; Ryan et al. 2013). For this reason, the 1995 Federal Wildland Fire Management Policy (updated in 2001), and 2014 National Cohesive Wildland Fire Management Strategy (updated in 2023) were implemented to guide fire management through collaborative efforts between federal and non-federal institutions.

In ecosystems dominated by ponderosa pine and dry mixed-conifer forests across much of the western US, resilient stand conditions were historically characterized by low levels of surface and ladder fuels, low density and competition, and old (>150 years), large, drought-tolerant trees (Arno et al. 1995; Hagmann et al. 2019; North et al. 2022). These pre-settlement forest structures were maintained by low-intensity fires that burned frequently in highly flammable forest understories characterized by fine fuels including herbaceous spp. and pine needles (Agee 1993). In dry, fire-prone forests prescribed fire programs that emulate the frequency of historical fire regimes have the potential to reestablish and maintain resilient stand conditions through a negative feedback mechanism. Restored ecological memory – which is defined as the persistence of information and material legacies after a disturbance, influencing responses to future disturbances (Johnstone et al. 2016) – was evident in the Bob Marshall Wilderness (Montana, USA). There, two lightning-ignited fires occurring seven years apart shifted the stand structure back to open, mixed-conifer forests dominated by large ponderosa pines (Larson et al. 2013). However, other studies evaluating the negative feedback induced by previous burns at large landscape scale have found that the mitigating effect of reburns on burn severity decays over time (Parks et al. 2014b) and can be reduced by extreme fire weather conditions (Parks et al. 2015a).

Where current forest structure and fuel accumulations are substantially departed from historical conditions, fuel reduction treatments are employed to restore historical fire regimes, support forest resilience by mitigating fire behavior (Agee and Skinner 2005), and potentially reduce fire suppression efforts and costs (Agee et al. 2000; Moghaddas and Craggs 2007; Urza et al. 2023). The effectiveness of site-level treatments has been extensively studied (Fulé et al. 2012; Kalies and Yocom Kent 2016; Davis et al. 2024) and assessed in the context of varying

topographic, climatic, weather, and fuel conditions (Cansler and McKenzie 2014; Prichard et al. 2020; Cansler et al. 2022). While prescribed fire alone may be effective at mitigating burn severity by reducing ladder and surface fuels (Vaillant et al. 2009), prior thinning may be necessary in high-density stands to restore resilient horizontal structure, and prevent or at least reduce crown fire risk (Agee and Skinner 2005; Urza et al. 2023). The general agreement is that fuel treatments that combine thinning followed by prescribed fire are the most effective (Hudak et al. 2011; Prichard and Kennedy 2014; Prichard et al. 2020, 2021; Cansler et al. 2022). Despite extensive literature documenting the mitigating effects of fuel treatments on burn severity, understanding their role amid other wildfire drivers remains a complex challenge. This difficulty largely stems from limited pre-fire fuel data, varying weather conditions during a wildfire, and a lack of studies incorporating experimental designs (but see Brodie et al. 2023). Additionally, there is a knowledge gap related to the compounding effects of firefighting operations and fuel treatments on burn severity (but see Harris et al. 2021).

The Bootleg Fire was ignited by lightning in July 2021. It burned a total of 413,766 acres over 41 days in the Fremont-Winema National Forest, in south-central Oregon. The wildfire had a profound impact on the Klamath Tribes' ancestral homeland, causing ecological and cultural damage, as well as loss of natural resources. The Bootleg Fire was the third-largest fire in Oregon's history since 1900, and it exhibited extreme fire behavior, resulting in extensive high burn severity (C. Chamberlain et al., University of Washington, Seattle, Washington, USA, unpublished data). As described by a spokesperson for the Oregon Department of Forestry, "The fire is so large and generating so much energy and extreme heat that it is changing the weather, […] normally the weather predicts what the fire will do. In this case, the fire is predicting what the weather will do" (Fountain 2021).

In a recent study, C. Chamberlain et al. (University of Washington, Seattle, Washington, USA, unpublished data) developed and applied a remote sensing-based analytical framework to identify key drivers of burn severity and to assess the effectiveness of fuel treatments in moderating burn severity across the Bootleg Fire footprint. This and other studies (Kane et al. 2015a; Parks et al. 2018b; Povak et al. 2020; Prichard et al. 2020; Cansler et al. 2022) have widely investigated drivers of burn severity at the fire-scale using ensemble machine learning (ML) models. However, few studies to date have examined drivers of burn severity at a local scale, evaluating how they might vary spatially while accounting for their interactions (but see Povak et al. 2020).

In this study, we evaluated how past fuel reduction treatments influenced burn severity within the 1800-ha area near the Sycan Marsh Preserve located in the northeast corner of the Bootleg Fire. Treatments aiming to restore resilient forest structure and wildlife habitat were conducted over the 16 years preceding the wildfire, including mechanical thinning (Tx), prescribed fire (Rx), and both treatments combined (TxRx). Although our study area covers only a section of the Bootleg Fire as constrained by the availability of pre-fire LiDAR data, it provides the opportunity to closely investigate burn severity across a complex landscape characterized by undulating landforms hosting dry forest (treated and untreated), riparian, and wetland ecosystems. Furthermore, our study area, which burned under nearly identical severe fire weather conditions, provides an excellent opportunity to evaluate the spatial variation in how different environmental variables, fuel treatments, and firefighting operations influenced burn severity. The size of the study area and the unusually detailed information on fuel and fire management provided by The Nature Conservancy (TNC) allowed us to investigate burn severity variability closely while leveraging highly reliable information that is commonly not available at

the wildfire scale. We gathered information about the impact of fuel treatments on firefighting operations from the fire program manager who was on-site during the wildfire, and incorporated suppression efforts into our analysis.

Through this study, we aimed to quantify the effectiveness of fuel treatments while addressing research gaps related to their impact among other burn severity drivers and evaluating how various predictors affected burn severity at a local scale, while accounting for their interactions. We pursued the following objectives:

1. Assessing the distribution and variability of burn severity across different fuel treatments and untreated forests.
2. Evaluating and explaining the impact of the most important environmental drivers as well as fuel treatments and firefighting operations on burn severity, and how their local effect varied spatially across our study area.

This study contributes to the body of knowledge by providing a reproducible framework to explain the effect of contagious processes like fire at both global and local scales. Additionally, it provides valuable lessons to guide and improve fire and fuel management practices across multi-ownership landscape.

Methods

Study area

Our study area is located in the Fremont-Winema National Forest, southcentral Oregon, USA. It matches the extent of pre-fire LiDAR (2018) data, covering a portion of the Bootleg fire that burned under severe fire weather conditions into one larger and two smaller LiDAR coverage parcels (Figure 1). Elevation ranges between ~1518m and ~1676m. Climate is characterized by cold, snowy winters, and hot, dry summers (Agee 1993). Based on 1991-2020

climate normals (Wang et al. 2023), mean annual precipitation and precipitation as snow are 531 mm and 115 mm, respectively, and mean annual temperature is 7 °C, ranging from 26 °C in summer and -6 °C in winter. The forest is dominated by ponderosa and lodgepole pine (*Pinus ponderosa* and *P.contorta*). Understory vegetation includes bitterbrush (*Purshia tridentata*), *Ceanothus* spp., manzanita (*Arctostaphylos spp.*), kinnikinick (*Arctostaphylos uva-ursi*), quaking aspen (*Populus tremuloides*), and willow (*Salix* spp). Historically, the Fremont-Winema NF was predominantly composed of large and old ponderosa pines, and the fire regime was characterized by frequent, low intensity fires (Agee 2003; Hagmann et al. 2013).

Over the past 16 years, the study area has been co-managed through a collaborative partnership between The Nature Conservancy (TNC), The Klamath Tribes, and the USDA Forest Service. The goals driving fuel treatments included the restoration of historical forest composition by recreating spatial complexity, a frequent and low-intensity fire regime, forest functions to support wildlife, and understory vegetation critical for tribes. Additionally, one of the goals was to create a safe environment for fire training programs. In our study area, fire and fuels managers have implemented 41 treatment units including mechanical thinning (Tx, 7% of total area), prescribed fire (Rx, 32% of total area), and thinning followed by prescribed fire (TxRx, 51 % of total area).

For our study, untreated areas were considered as a single untreated unit (10% of the total area). Thinning was conducted between 2012 and 2017, except for one unit that received thinning in 2005, and prescribed fire was conducted between 2008 and 2021. In most Tx units, thinning was employed to restore wildlife habitat, and resilient forest structure and composition using Individuals, Clumps, and Openings (ICO, Churchill et al. 2016) prescriptions. Trees were harvested using a disc saw, followed by whole-tree yarding to transport the entirety of each tree

to the landings. There, delimbing occurred, resulting in the accumulation of slash piles. These piles were subsequently burned as a preparatory step before prescribed fire. The entire harvesting process took place from December to March to protect soils by working on frozen ground with snow. Where appropriate, Rx was applied on its own to reduce overstory tree density through thermal thinning (stem and crown scorching). In Rx and TxRx units, based on information provided by TNC and as shown in the 2020 National Agricultural Imagery Program (NAIP, 0.6 m) mosaic (Figure 3), post-treatment burn severity was heterogeneous, reflecting variable fuel conditions, and ignition patterns. Local managers estimated that average tree mortality after prescribed fire was less than 5% across the treated area. Some areas less than 2 ha had more than 5% tree mortality (Figure 2). Rx was applied from 2008 to 2019 expect for unit 8, which was burned in 2017, and then again in 2021.

The Bootleg Fire was ignited by lightning on July 6, 2021. MODIS active fire mapping (Giglio et al. 2009) indicated it burned through our study area from July 13 to July 21, progressing with the prevailing wind direction from southwest to northeast. During days of burning, fire weather was characterized by low fuel moisture and relative humidity, and high temperature and Energy Release Component (ERC) (Table 1). Based on these metrics, our entire study area burned under similar fire weather conditions. Maximum wind speed exceeded 20 mph on several days, reaching 40 mph on July 18 for a short period of time. On that day, local managers observed extreme fire behavior, including a fire-tornado which uprooted several trees (Figure 2, D).

Burn severity data

Burn severity is defined as a "scaled index gauging the magnitude of ecological change caused by fire" (Key and Benson 2006). The Composite Burn Index (CBI) is a common ground measurement of burn severity that aggregates post-fire effects (Key and Benson 2006) and is

used to validate satellite-derived burn severity observations (e.g., Prichard et al. 2020). The CBI scale ranges from 0.0 to 3.0, and is divided into four classes including no-effect (0.0), low (0.5-1.0), moderate (1.5-2.0), and high severity (2.5-3.0).

Following methods described in Howe et al. (2022) and Parks et al. (S. Parks et al. 2018) we calculated the Relativized Burn Ratio (RBR; Parks et al. 2014a) across the entire fire perimeter using Google Earth Engine (Gorelick et al. 2017), and then clipped it to the study area extent. We selected RBR over other indexes for two reasons: 1) Parks et al. (2014a) demonstrated that RBR better represents CBI measurements; 2) based on a comparison against burn severity distributions of the delta Normalized Burn Ratio (dNBR), relativized dNBR (RdNBR), and delta Normalized Difference Vegetation Index (dNDVI) by fuel treatment type, RBR had fewer outliers and best discriminated fuel treatment classes.

The index was computed using one-year pre- and post-fire mean composite imagery collected during the growing season (June 1 – September 30) to capture survivorship potential and delayed mortality (Key and Benson 2006) in response to the Bootleg Fire. Our 2020 mean composite imagery used to calculate RBR did not account for the possible effect of the pre-Bootleg Rx treatment conducted over unit 8 in 2021. However, given the very low burn severity observed in 2022 (after the Bootleg Fire; Fig. S5) – which indicates a small reflectance change between 2020 and 2022 – and the similar forest structure observed through a visual assessment of NAIP 2020 and 2022 (Figure S1), we decided to retain unit 8 in our analysis. Ground assessment of burn severity conditions is not always possible or in some cases it does not satisfy the number of samples necessary to infer a statistical relationship between CBI and satellite-derived burn severity observations. In our study area CBI observations were limited in numbers,

hence we used Parks et al. (2019, Table 7) RBR thresholds corresponding to CBI classes to interpret burn severity data.

We calculated RBR employing Sentinel-2 Level 2A surface reflectance data. Compared to Landsat 8 Operational Land Imager (OLI), Sentinel 2 Multispectral Instrument (MSI) has bands at higher resolution. The Near Infrared (NIR) and the Shortwave Infrared (SWIR 2) bands necessary to calculate RBR have a native resolution of 10 and 20 m respectively; to exploit the finest scale available, we created our burn severity raster at a pseudo 10 m resolution (Howe et al. 2022). Additionally, burn severity was further explored by visually inspecting pre- and post-fire imagery extracted from the National Agriculture Imagery Program (NAIP) collection. We downloaded 2020 and 2022 multispectral (red, green, blue, NIR bands) NAIP imagery at 0.6 m resolution using GEE (Figure 3, B).

Management data

We created a single fuel treatment vector layer by merging data provided by TNC with data extracted from the Interagency Fuel Treatment Decision Support System (IFTDSS 2021) database. The vector layer was then clipped to the extent of the 2018 LiDAR footprint, and areas found within the 2018 LiDAR boundary that did not receive any treatment were labeled as untreated. The larger and two smaller parcels of 2018 LiDAR coverage were treated as a single area for analysis purposes. Given the opportunistic nature of this study, and the limited extent of pre-fire LiDAR, we used the combined untreated areas as a control after verifying that forest types in untreated units matched those found in treated units based on the 2020 LANDFIRE (Ryan and Opperman 2013) Existing Vegetation Type dataset (EVT; https://landfire.gov/evt.php). The final fuel treatment vector layer included Tx, Rx, TxRx, and untreated classes. We collected firefighting operations data by requesting the local fire program manager to fill out the Wildfire Interactions with Treatments Survey (WITS) created by

Washington DNR (Anna Barros and Gretchen Engbring, Washington, USA, personal communication). We simplified those data into a single variable for analysis, representing the presence or absence of fire suppression by treatment unit.

LiDAR-derived forest structure and topographic metrics

We obtained 2018 pre-fire LiDAR data from USFS and 2021 post-fire LiDAR from the open source USGS server (USGS LiDAR 2021). Mean first returns per square meter were 11 and 15 respectively. We used FUSION/LDV LIDAR Analysis and Visualization software version 4.51 (McGaughey 2020) to calculate forest and topographic metrics at 30 m and 15 m resolution, respectively. Pre-fire LiDAR was collected before some of the prescribed fire treatments were conducted. For this reason, we did not include metrics representing lower fuel strata, and forest metrics were computed using exclusively first returns, with a 2-m cutoff to limit the inclusion of understory vegetation while accounting for the presence of saplings. Forest metrics included canopy cover, mean canopy height, canopy base height, standard deviation canopy height, and canopy rumple (Parker et al. 2004).

We also computed LiDAR-derived ICO metrics (LICO) to quantify individual trees (1-tree clump canopy), tree clumps (1-tree clump canopy, 2-to-4-tree clump canopy, 5-to-9-tree clump canopy, 10-plus-tree clump canopy), and openings (canopy core gap) (Churchill et al. 2016). LICO metrics representing individual trees and tree clumps correspond to the percentage of the canopy area in each 30-m pixel, in clumps of different sizes; openings correspond to the percentage of the area at least 6 m from the nearest canopy. This measure indicates the presence of very large gaps.

Topographic metrics included aspect, elevation, curvature, plan curvature, profile curvature, slope (moving windows: 15 m, 45 m, 135 m, 270 m), solar radiation index (SRI), and topographic position index (TPI; moving windows: 200 m, 500 m, 1000 m, 2000 m, 4000 m).

We computed these metrics using post-fire LiDAR data given its greater extent compared to pre-fire LiDAR data. For instance, to calculate topographic position index with a 4000-m moving window, a 4000-m radius in all directions was required with respect to each pixel within the study area (as delimited by the pre-fire LiDAR footprint). Methods used to calculate forest and topographic LiDAR-derived metrics are detailed in the FUSION/LDV manual (McGaughey 2020).

Weather data

We calculated wind metrics using wind data computed with WindNinja software version 3.8 (Forthofer 2007) and extracted other daily fire weather variables from the University of Idaho Gridded Surface Meteorological (GRIDMET; Abatzoglou 2013) dataset available in GEE. Hourly-interpolated, topography-driven wind vectors were calculated for each fire day, following directions detailed in WindNinja's tutorial 3 (https://weather.firelab.org/windninja/tutorials/). Using the Point Initialization option, we selected weather stations within a 10-km buffer around the study area. We used wind speed, and wind direction vectors produced at 90-m point spacing, to derive daily maximum wind speed, and related ordinal eastwestness (sine transformed radians) and northsouthness (cosine transformed radians) direction layers. GRIDMET layers (4-km resolution) considered in this analysis were energy release component, fuel moisture (100 and 1000 h), vapor pressure deficit, maximum temperature, and minimum relative humidity. Infrared imagery-derived heat perimeters were obtained from the 2021 National Infrared Operations (NIROPS; USDA 2021) dataset for most days throughout the entire wildfire progression. Daily wind and GRIDMET layers were intersected with NIROPS perimeters to create 10-m raster layers capturing weather variability based on daily wildfire progression.

We produced snow cover metrics using MODIS/Terra Snow Cover Daily L3 Global 500-m SIN Grid (Version 6) dataset, and by running the GEE script provided by Crumley et al.

(2020). Snow cover metrics (500 m) included snow cover frequency (the % of days a pixel is covered in snow during the water year), and snow disappearance date. The Level-4 Evaporative Stress Index (ESI; Fisher 2018), calculated using the Priestley-Taylor Jet Propulsion Laboratory (PT_JPL) algorithm, was obtained by following tutorials published on the ECOSTRESS homepage (https://ecostress.jpl.nasa.gov). ECOSTRESS-derived metrics are calculated using the thermal infrared brightness temperature of plants collected from the space station. ESI is a drought index ranging from 0-1 (0 being water stress, 1 being no water stress) calculated as the ratio of evapotranspiration (i.e., water used by plants; ET) over potential evapotranspiration (i.e., maximum rate of atmospheric demand; PET). Both ET and PET are ECOSTRESS-derived metrics. The ESI layer used in this analysis was derived from data collected on July 10, 2021, just 3 days before the Bootleg Fire approached our study area, according to NIROPS. Additionally, we obtained Incident Action Plans fire weather data from TNC. This dataset, which was provided as a summary table (Table 1), was used to interpret our results, since it offered critical information to understand fire weather conditions observed on the ground.

Climate data

Climate layers, including 1981-2010 actual evapotranspiration (AET) and 1981-2010 climatic water deficit (CWD) grids were calculated following methods described in Appendix B of Cansler et al. (2022). AET represents the amount of photosynthesis that can occur given available water (i.e., realized site productivity). In contrast, WCD represents the amount of evaporative demand that cannot be met due to dry conditions (i.e., moisture stress). ClimateNA software (Wang et al. 2016) was used to compute other climatic normals (1991-2020), including Hargreaves climatic moisture deficit (representing the difference between reference evapotranspiration and monthly precipitations), mean annual precipitation, May-September precipitation, and precipitation as snow. This software computes metrics by downscaling 1991-

2020 PRISM gridded monthly climate normals (928 m resolution) to scale-free point locations at 90-m distance for all North America.

Vegetation data

To evaluate the possible effect of different vegetation types on burn severity, we downloaded the Fire Resistance Score (FRS; Stevens et al. 2020) and the 2020 LANDFIRE EVT using LF Map Viewer (www.landfire.gov/viewer/). FRS is a summary of functional traits of fire-adapted conifer tree communities used to quantify the resistance of forest communities to tree-killing fire. It is derived from species-specific traits related to morphology and litter flammability. EVT represents associations of plant community types that are commonly found within landscapes featuring similar substrates, ecological processes, and/or environmental gradients. EVT maps are created using decision tree models, field data, Landsat imagery, elevation, and biophysical gradient data. Given the dominance of the ponderosa pine forest, woodland and savanna forest type (57%), and the relative low cover of all other vegetation classes (< 5% each), the EVT layer was re-coded as a binary variable representing dominant and non-dominant vegetation.

Distance to streams and wetlands data

To capture the possible effect of riparian and wetland ecosystems on burn severity within our study area, we created a distance-to-streams-and-wetlands layer. We sourced wetlands data from the Oregon Department of State Lands Statewide Wetlands Inventory (ODSL 2021), and whole stream routes from the Oregon Department of Fish and Wildlife data clearinghouse (ODFW 2021). After merging and rasterizing the geospatial datasets, we calculated the distance for each pixel using the R function `distance` from the `raster` package (version 3.6-20).

Data frame building

All layers used in this analysis were either vector shapefiles or rasters. In order to build a comprehensive and coherent dataset, all shapefiles were rasterized matching the extent and projection of the RBR raster. The statistical methods employed in this study are limited to numeric variables – whether binary, discrete, or continuous. For this reason, we recoded variables that represent multiple classes into binary variables. EVT classes were simplified to dominant (1) and non-dominant (0) vegetation types. The fuel treatment layer, originally representing four classes (i.e., Tx, Rx, TxRx, and untreated), was recoded into two binary variables: Tx and Rx. These variables indicate the presence (1) or absence (0) of these treatments. This reduction was driven by the aim to limit the dimensionality of our data frame, decrease data sparsity (i.e., increase the proportion of non-zero observations), and enhance model interpretability. The choice of including fuel treatments in the model was to account for variable surface fuel loads, with the expectation that units treated with prescribed fire had lower fuel accumulation in those strata.

We used raster value extraction via point sampling with reprojection to build our data frame following a series of steps: 1) creating a point layer with point locations evenly spaced at 90-m distance to reduce the effects of spatial autocorrelation (see Objective 2 in the Analysis section); 2) iteratively extracting raster values using point location after reprojecting the point layer to the raster being sampled; 3) merging all values extracted from each raster into a single data frame. This method allowed us to build a dataset that pulled values from a wide range of variables, thus avoiding the intrinsic error associated with the direct resampling of rasters. We retained only entries with canopy cover > 10% (as determined from the pre-fire LiDAR) to make sure our analysis focused on forested ecosystems. We chose to use a 10% threshold based on the

Forest Inventory and Analysis Program (FIA) definition of forest. We then validated this threshold through visual assessment of 2020 NAIP imagery covering our study area.

The initial data frame included > 50 variables, which had to be reduced before running our statistical analysis. We conducted a two-step reduction as follows: 1) retaining only predictors that had a Spearman correlation coefficient < 0.6 and that were more highly correlated with RBR; 2) recursively eliminating features (i.e., backwards selection) with Random Forests, optimizing for a higher variance explained. Recursive feature elimination (RFE) was conducted using the function `rfe` from the `caret` package (version 6.0-94; Kuhn 2008). Step 1 reduced the list of variables down to 23, while step 2 reduced the list down to 16, removing also mechanical thinning. However, given our interest in understanding the local effect of fuel treatments on burn severity, we retained mechanical thinning. The final data frame included 17 predictors (Table 2) and 1846 observations.

Analysis

Objective 1: Burn severity assessment

To evaluate the influence of fuel treatments on burn severity and capture its variability within each treatment class, we created violin plots showing the distribution of burn severity by fuel treatment type (untreated, Tx, Rx, TxRx), and by individual units, respectively. CBI thresholds derived specifically for RBR were used to quantify the percentage of area burned at low (≤ 135), moderate (136-300), and high (≥ 301) severity for each treatment class (Parks et al. 2018a).

Objective 2: Random Forests and SHAP analysis

We developed a Random Forests regression (RF; Breiman, Leo 2001) model with an explanatory focus and applied SHapley Additive exPlanations (SHAP; Lundberg & Lee 2017; Molnar 2023) analysis to uncover both the global impact and the local effect of predictors

influencing burn severity. Our model utilized the complete dataset of 1846 observations, prioritizing a comprehensive understanding of burn severity variations within our specific study area over predictive accuracy on new, unseen data.

We ran the entire analysis using R programming language (RStudio Team 2020). Functions from the `tidymodels` framework (version 1.1.0) were used to build our modeling workflow and the `ranger` package (version 0.15.1; Wright and Ziegler 2017) was used to train the RF model. Hyperparameter tuning was systematically evaluated through 10-fold cross-validation to determine how different number of features considered for splitting at each node (mtry) and the minimum number of observations required to form a new node in a tree (min_n) performed, based on the pseudo-R^2 metric. The best parameters (mtry = 4, min_n = 5) were then used to train the final RF model. Subsequently, we employed the `DALEXtra` package (version 2.3.0; Maksymiuk et al. 2021) to evaluate the model performance, and extract predicted values and residuals. Given that the contagious effect of fire spread is inherently a spatial process, we assessed the possible presence of spatial autocorrelation in the residuals to verify that our model did not violate the assumption of independence. Our assessment involved creating a Moran's I plot with a lag distance of 90 m (representing the sampling distance) by using the `correlogram` function in the `elsa` package (version 1-1.28; Naimi et al. 2019).

SHAP analysis is a statistical approach based on Shapley values, a method from the coalitional game theory employed to explain black-box models such as RF (Lundberg et al. 2019). While a coalition in a game represents a group of players, a coalition in a black-box model represents a group of features (i.e., predictors). After evaluating the contribution of each feature value to a predicted value across all possible coalitions, the average contribution of a feature value (i.e., Shapley value) is calculated. Based on this notion, SHAP analysis allows us to

understand 1) the local importance (effect) of each predictor value at the scale of a 90-m raster grid cell and 2) the global importance (impact) of each predictor. In our case, SHAP values represent the local importance of each feature value for the burn severity prediction of a specific data point. Specifically, they quantify the contribution of each feature value to the deviation from the mean prediction. Thus, for a specific prediction, the sum of the contributions of all feature values equals the deviation. SHAP global importance, instead, serves as an alternative to permutation feature importance commonly calculated in RF analyses. Unlike permutation importance, which is based on the decrease in model performance, SHAP global importance is calculated by taking the mean of the absolute SHAP values for each feature (e.g., Rx) across all the data points (i.e., 1846 observations). Essentially, it quantifies the overall impact of each feature on the model's predictions.

SHAP values can be positive or negative, indicating whether the effect of the feature value increases or decreases the predicted outcome, respectively. In the context of this study, a negative SHAP value would suggest that the feature value is associated with a decrease in the burn severity prediction, while a positive SHAP value would suggest an increase. The magnitude of SHAP values reflect the strength of the effect of each feature value on the prediction, with larger absolute values indicating a greater influence. We conducted SHAP analysis using the `treeshap` package (0.2.5; Yang 2022), and created a SHAP raster for each predictor at 90-m resolution, representing the sampling distance. Finally, we used raster layers to evaluate the spatial heterogeneity of each predictor influence and dependence plots to assess the overall trend of each predictor effect.

Results

Through the assessment of the spatial distribution and variability of burn severity across different fuel treatments and untreated areas, we found that the influence of fuel reduction on burn severity varied by treatment prescription. In units treated with Rx and TxRx, percentage of area burned at low severity was 86% and 83%, respectively; for both treatments, moderate and high burn severity accounted for less than 15% and 5% of the area burned. In contrast, in units treated with Tx, percentage of area burned at low, moderate, and high severity was 30%, 45%, 25%, respectively. Finally, in untreated forests, percentage of area burned at low, moderate, and high severity was 31%, 27%, 42%, respectively (Figure 4, A and B).

We used RF and SHAP analysis to evaluate the impact of top drivers as well as fuel treatments and firefighting operations on burn severity, and how their influence varied spatially across the study area. RF model performance reported an R^2 of 0.94 and a root mean square error (RMSE) of 31.8 for predicting RBR. The model fit revealed a mostly linear relationship between observed and predicted RBR values (Figure S2). Residuals spatial autocorrelation exhibited a Moran's I value that ranged between 0.1 and 0.0, indicating spatial independence in the residuals (Figure S2). Top predictors included Rx, ESI, 4-km window Topographic Position Index (TPI-4km), and canopy cover, in descending order of importance, while firefighting and Tx were ranked third-to-last and last, respectively (Figure 4, C).

The influence of each predictor's value on predicted burn severity varied spatially (Figure 6). Rx SHAP values ranged between -29 and 150. Observations indicating the implementation of Rx (Rx = 1) corresponded to lower predicted burn severity (negative SHAP values), whereas elsewhere (Rx = 0) corresponded to higher predicted burn severity (positive SHAP values) (Figure 5, A; Figure 6, A). Tx SHAP values ranged between -6 and 6. The distributions of

observations representing the presence of Tx (Tx = 1) and its absence (Tx = 0) revealed a nuanced effect on predicted burn severity. Some areas treated exclusively with Tx were associated with marginally higher predicted burn severity, and some that were untreated (Tx = 0, Rx = 0) exhibited lower predicted burn severity. Firefighting SHAP values ranged between -13 and 13 (Figure 5, F; Figure 6, F). Firefighting efforts that were conducted in units treated with Rx were associated with a decrease in predicted burn severity. Where Rx was absent, firefighting operations were linked to both a marginal increase and decrease in predicted RBR. Areas where firefighters did not intervene (Firefighting = 0) were subjected mostly to higher predicted burn severity (Figure 5, E; Figure 6, E). However, the magnitude of the influence of this variable remained consistently low compared to top predictors.

ESI SHAP values ranged between -68 and 97, showing a positive increasing trend with increasing ESI values, ranging between 0.4 to 0.7. Areas experiencing lower water stress were associated with higher predicted RBR (Figure 5, B; Figure 6, B). TPI-4km SHAP values ranged between -54 and 152, showing a steep negative slope between -4000 and 0 TPI-4km. The trend then plateaued over the 0-8000 TPI-4km range. Valleys, represented by more negative TPI-4km values, were positively correlated with increasing predicted RBR, while those representing hills and ridges (more positive TPI-4km) were associated with lower burn severity (Figure 5, C; Figure 6, C). Additionally, exploratory analysis disclosed a strong, negative correlation (Spearman = -0.80) between TPI-4km and Hargreaves' climatic moisture deficit (CMD; Figure S3) averaged over 30 years (1991-2020). Canopy-cover SHAP values ranged between -39 and 102, showing a positive, mostly linear relationship with observed canopy cover. Pixels featuring > 40% canopy cover were associated with increasing burn severity. (Figure 5, D; Figure 6, D).

Discussion

Due to the unpredictability of where and when wildfires burn, burn severity studies that include experimental designs and pre-fire fuel characterization are rare (but see Brodie et al. 2023). Where pre-fire field datasets are not available, LiDAR data can be invaluable to represent pre-fire fuel conditions (Andersen et al. 2005). In this study, we evaluated drivers of burn severity within a section of the 2021 Bootleg Fire by leveraging pre-fire LIDAR data, reliable fuel and fire management datasets, and a curated selection of environmental variables. Untreated forests and Tx units burned predominantly at high and moderate severity, respectively. In contrast, both Rx and TxRx units burned mostly at low severity (Figure 4, A and B).

Based on SHAP values, prescribed fire was the most important driver of burn severity (Figure 4, C), followed by ESI, TPI-4km, and canopy cover. The impact of these variables on burn severity was at least 5-fold larger than that of firefighting operations (Figure 4, C). Finally, the effect of thinning on its own had a negligible impact on predicted burn severity, although overall, Tx units exhibited lower observed burn severity than untreated forests (i.e., Tx showed a higher percentage of area burned at moderate severity and a lower percentage of area burned at high severity).

Burn severity assessment and fuel treatment effectiveness

The Bootleg Fire burned through the study area over a period of eight days, progressing from southwest to northeast. Fire weather conditions were consistently severe (Table 1), allowing us to isolate the effect of fuel treatments and other covariates on burn severity. As encountered in other case studies (e.g., Murphy et al. 2007; Rogers et al. 2008), the rate of fire spread decreased in most of the treated units. According to the TNC fire manager (K. Sauerbrey, The Nature Conservancy, Oregon, USA, personal communication), reduced fire intensity and

flame length were observed as the fire burned into the treated forests. We observed a substantial difference in percentages of area burned at low, moderate, and high severity between units that were treated with prescribed fire and those that were not, suggesting that likely fire behavior and consequent burn severity varied in response to fuel structure and accumulation (Agee and Skinner 2005; Vaillant et al. 2006; Ritchie et al. 2007; Safford et al. 2009, 2012). The area within Rx and TxRx units burned predominately at low severity (> 80%). In contrast, Tx units and untreated forests were predominantly characterized by moderate (45%) and high (41%) severity burns, respectively (Figure 4, B). However, we observed patches of low burn severity in untreated, freshwater forested-shrub wetlands near units 13 and 1 (Figure 1), where moister soil provided a refuge for encroaching trees against the spread of fire.

Treated units facilitated burnout and direct attack operations, providing safer zones for firefighters (K. Sauerbrey, The Nature Conservancy, Oregon, USA, personal communication; Harbert et al. 2007). Rx units were particularly suitable, having been previously used for fire training programs in collaboration with The Klamath Tribes. Where fire suppression occurred, we observed a decreasing trend in predicted burn severity within units treated with Rx and more variable effects within Tx units (Figure 5, E). Notably, units 44 and 15 were the only Tx units used in firefighting operations. In unit 44, direct attack and burnout operations successfully suppressed the wildfire, resulting in low burn severity. Conversely, in unit 15, despite direct attacks holding the Bootleg Fire for over 24 hours, the fire eventually gained momentum to the west burning through untreated forests and then crossed the fire lines as a crown fire, leading to a mix of burn severities. Specifically, in panel E, Figure 6, where firefighters intervened (firefighting = 1) within Tx treatments (Rx = 0), unit 15 reported variable effects; conversely, unit 44 reported exclusively decreasing predicted burn severity. Contrary to findings by Harris et

al. (2021), showing a 72% reduction in burn severity through a combination of prescribed fire and firefighting, our burn severity assessment indicated predominantly low burn severity within units treated with Rx regardless of whether firefighting operations were conducted. While SHAP analysis revealed that the impact of firefighting operations on predicted burn severity was small across different types of treatments, we believe that its local effect was underestimated in Tx unit 44, where firefighters suppressed the wildfire with burnout operations.

Our findings on the effectiveness of fuel treatments largely corroborates results from prior research on fuel treatment effectiveness. Studies have shown that fuel treatments including prescribed fire were more effective at mitigating burn severity than thin only treatments (Prichard and Kennedy 2014; Yocom Kent et al. 2015; Prichard et al. 2020; Cansler et al. 2022), and that effectiveness declined as treatment age increased (Finney et al. 2005; Hudak et al. 2011). Moreover, in three reviews, it was found that thinning followed by prescribed fire was consistently the most effective treatment, and that, in comparison, Rx and Tx alone were either less effective (Fulé et al. 2012; Davis et al. 2024) or led to mixed results (Kalies and Yocom Kent 2016). Differences in burn severity between units treated with prescribed fire and those without can likely be attributed to surface fuel reduction in Rx treatments compared to potential increases in surface fuels through Tx treatments (Vaillant et al. 2006; Knapp et al. 2017). Although we could not conduct pre-Bootleg fuel surveys in our retrospective study, consultations with the local manager (C. Bienz, The Nature Conservancy, Oregon, USA, personal communication) indicated that Rx and TxRx units had lower fuel loads compared to untreated forests and Tx units. Therefore, we interpreted the occurrence of prescribed fire as a proxy for pre-fire fuel accumulation in the lower strata, leveraging the recent timing of this prescription (<5 years, except for one unit treated in 2008).

Prescribed fire disrupts both vertical and horizontal fuel continuity by consuming accumulated biomass (Agee and Skinner 2005; Reinhardt et al. 2008), thus limiting crown scorch and tree mortality even under extreme weather conditions (Prichard and Kennedy 2014; Yocom Kent et al. 2015; Povak et al. 2020; Prichard et al. 2020; Brodie et al. 2023). This mechanism was evident in our study area where Rx and TxRx units showed lower burn severity. In contrast, Tx units where fire suppression was not conducted or successful featured mostly moderate and high severity burns. Extensive crown scorch, and torching may have been caused by increased surface fuels from logging slash, fuel aridity, and wind speed, resulting from thinning (Agee and Skinner 2005; Whitehead 2008; Ma et al. 2010; Kane 2021) and exacerbated by hot summer temperatures. Despite being less effective than treatments including Rx, thinning was still more effective than untreated forests according to RBR observations. Likely, untreated forests were more susceptible to crown fire than thinned units due to differences in forest structure. Specifically, LiDAR-derived metrics revealed lower mean canopy height, canopy base height, horizontal and vertical canopy complexity, and higher canopy cover where forests were untreated (Figure S4).

Despite the broad trends indicating the effectiveness of treatments, we observed local variability in burn severity across both treated and untreated forests. Although fire severity was generally lower in Rx and TxRx units, we also observed patches of high severity burns within units treated with prescribed fire. This was particularly evident in areas featuring one or a combination of the following conditions:

1. controlled burns were not applied consistently, especially near riparian zones (Figure 1, unit 20) where fuel was not treated to avoid potential negative impacts on the riparian system (Stone et al. 2010), and soil was drier due to hot summer temperatures;

2. canopy cover was continuous and exceeded 40%;
3. Rx alone was conducted 13 years prior to the Bootleg Fire.

For instance, the TNC fire manager informed us that post-thinning fuel found in the northeast corner and other areas within TxRx unit 20 was not treated with prescribed fire; rather, it was piled and burned. The presence of residual slash coupled with drier fuel conditions, high canopy cover (>40%), and the advance of high intensity fire from the adjacent untreated unit, likely contributed to the high severity noted in that area (RBR > 450). Moreover, unit 20 was characterized by a riparian zone dominated by fire-sensitive species including willows and lodgepole pines, which burned at high severity (Figure 2, E). We also observed patches of high and moderate burn severity in Rx unit 11, where prescribed fire was conducted 13 years prior to the Bootleg Fire. This unit experienced a mountain pine beetle (*Dendroctonus ponderosae* Hopkin; Bentz 2008) outbreak in 2008, affecting both lodgepole and ponderosa pines. Due to the low timber prices, that year TNC opted to use prescribed fire as a method to reduce stand density, thereby decreasing the vulnerability of the remaining pines to drought stress and further insect attacks. When the wildfire burned into unit 11, it likely encountered young trees sensitive to fire, as well as snags and surface fuels from the death of trees following the insect outbreak and prescribed fire, resulting in moderate and high severity burns (Agee 2003; Schoennagel et al. 2012).

Our burn severity assessment and the marginal local effect of thinning quantified through SHAP analysis revealed that prescribed fire alone can be as effective as combined thinning and burning treatments. This approach has both economic and ecological implications for forest managers. Specifically, where conditions exist to allow Rx on its own and where commercial thinning cannot offset treatment costs, Rx can be a more cost-effective method than TxRx

(Holland et al. 2022). Tx treatments may also have higher environmental impacts than Rx, including risks of soil disturbance and compaction and injuries to live trees (Picchio et al. 2020). Over time, repeated application of Rx can act as a thinning agent by killing small trees, creating more canopy openings, and increasing canopy base height. However, reintroducing fire through controlled burning (without thinning) in fire-excluded forests may pose substantial risks, including higher, undesired tree mortality due to high severity burns caused by abundant pre-fire fuel accumulation (Miller and Urban 2000), and recruitment of surface fuels through post-fire tree mortality (Agee 2003). Based on site-specific knowledge, we found that Rx units included some small pockets of high severity prior to the Bootleg Fire. However, this was a much smaller loss compared to the extensive tree mortality observed in Tx units and untreated forests due to the Bootleg Fire.

The role of top drivers on predicted burn severity

In our study area, the most important drivers of burn severity included ESI, TPI-4km, and canopy cover, all of which varied locally. Similarly to Birch et al. (2015), we found that canopy cover was the most important forest structure metric influencing burn severity. Canopy cover over 40% (Figure 5, D) was associated with increasing predicted burn severity across the study area; however, by overlapping maps of SHAP values for each predictor, we observed that moderate and high severity burns were confined to pixels characterized also by higher ESI (> 0.5, representing less water-stressed vegetation) and negative TPI-4km values (representing valleys and flatter terrain). Visual assessment of the spatial distribution of ESI and TPI-4km SHAP values, along with the fuel treatment map (Figure 1) and 2020 NAIP imagery (Figure 3, B), revealed a relationship between the spatial arrangement of the different treatments, forest structure, and the heterogeneous influence of each predictor. We observed that most of the

positive, large ESI and TPI-4km SHAP values – indicating higher predicted burn severity – were place-specific, including:

1. untreated areas (unit 43, except for the south-east corner of the main island representing a wetland area);
2. areas treated solely with Tx (unit 36, 37, 15), or where Rx was conducted in a non-uniform fashion, and included a riparian area (unit 20);
3. Rx units characterized by higher and more continuous, and higher canopy cover (e.g. unit 29, 6, 3, 4, and 28) compared to other units.

ESI is a drought indicator ranging from zero (high water stress) to one (low water stress), derived from thermal infrared brightness as captured by the ECOSTRESS mission (Fisher 2018). Based on a literal interpretation of our results, less water-stressed vegetation seemed to be conducive to moderate/high burn severity. However, through visual assessment of pre-Bootleg NAIP imagery, we observed a consistent relationship between horizontal fuel structure and ESI, which led us to an alternative explanation. Specifically, areas with green, denser, and more continuous vegetation cover were characterized by ESI values > 0.5; whereas areas with green, sparser vegetation cover were characterized by ESI values < 0.5 (Figure 3, C). These fuel patterns – coupled with the notion that ESI is not capable to discriminate vegetation from soil, and that soil temperatures are generally higher than those of vegetation – suggested that lower ESI values (indicating higher water stress) may have resulted from soil temperatures disproportionately influencing ESI estimates. Therefore, in this specific context, it is reasonable to consider ESI as a proxy for forest structure, and state that higher, more continuous vegetation cover was associated with moderate and high severity burns (Agee and Skinner 2005; Vaillant et al. 2006; Ritchie et al. 2007; Safford et al. 2009, 2012).

Considering our relatively small study area, the substantial impact of TPI-4km was initially unexpected. Coarse scale TPIs (2km window or greater) are typically more reflective of conditions over larger landscapes (Dillon et al. 2011; Kane et al. 2015a; Harris and Taylor 2017), capturing variation in fuel distribution and bioclimatic factors (e.g., AET), occurring at coarse spatial scales (Dillon et al. 2011; Kane et al. 2015b). Some studies have also indicated that TPI importance was less substantial when the effect of explicit (e.g., canopy cover) or implicit (e.g. fuel treatments) fuel-related variables were included in their analyses (Birch et al. 2015; Parks et al. 2018b; Povak et al. 2020; Prichard et al. 2020). In our study area, the strong influence of coarse-scale TPI was explained by variation in fuel structure and accumulation dictated by fuel treatments, as well as climatic moisture deficit affected by undulating landforms (Hargreaves and Allen 2003; Wang et al. 2016).

The strong negative correlation we found between TPI-4km and 1991-2020 CMD normal (Figure S3) corroborates the potential influence of TPI on microclimate (Ma et al. 2010). The occurrence of higher CMD coupled with negative TPI-4km values (Figure 3, D and E) indicated the existence of persistent drier conditions in valleys and on flatter terrain, where accumulation of live and dead fuel was higher. Negative TPI-4km identified areas characterized by moderate and high severity burns including untreated forests, Tx units, and Rx areas where slash from thinning was piled and burned instead of being underburned (unit 20). It is conceivable that valleys with denser vegetation (e.g., units 36, 37, 20, and untreated areas next to them) and flatter areas with sparser tree canopies (e.g., unit 15) experienced higher CMD, although for distinct reasons. In the first case, the higher CMD may have resulted from higher potential evapotranspiration with respect to precipitations (Wang et al. 2016). In the second case, higher

soil temperatures may have led to increased evaporation rates, contributing to a higher CMD (Ma et al. 2010).

Delayed post-fire tree mortality

We conducted our extended burn severity assessment one-year post fire to capture survivorship potential and early delayed mortality (Key and Benson 2006). However, delayed tree mortality will continue to manifest over several years and depend on complex factors that are difficult to predict. As shown in a study evaluating broadscale post-fire effects five to seven years after the fire (Miller et al. 2016), both increases in mortality and snag falls occurred across all burn severity classes. Evaluating whether a tree could have survived fire injuries years after a single or multiple fires (e.g., Rx + Bootleg) is challenged by many interacting stressors occurring before and after fire (Kane et al. 2017). Common stressors mediating tree death include pathogens (Parker et al. 2006), bark beetles (Kelsey and Joseph 2003; Hood et al. 2010; Prichard and Kennedy 2014), drought, and competition (Van Mantgem et al. 2013, 2018). Delayed tree mortality is consequently determined by complex relationships existing between biotic and abiotic agents, resulting in patterns of mortality similar to those observed in unburned forests (Das et al. 2016; Hood et al. 2018). In years following the Bootleg fire, subsequent tree mortality will depend on the interplay of burn injuries and ecological disturbances (e.g., drought, insect outbreaks, pathogens). With greater time since fire, attributing post-fire tree mortality to burn severity becomes a more complex and nuanced endeavor, further challenging our capacity to interpret and weight contributing factors.

Uncertainties

Satellite-derived indices are intrinsically uncertain given their coarse resolution and limited ability to capture and distinguish a wide range of biophysical characteristics (Furniss et al. 2020), such as fine-scale heterogeneity of fire effects, age and size of trees, and vegetation

types. Burn severity indices quantify change on a continuous scale, and are derived from the differencing of pre- and post-fire imagery (single or composite). The biophysical complexity existing on the ground is reduced to a single value originating from the average spectral reflectance assigned to each pixel. Therefore, numerous small dead trees could produce the same reflectance value as a single, large dead tree (Furniss et al. 2020), despite their vastly distinct impact on ecosystem functions and carbon cycling (Lutz et al. 2018). Additionally, large tree canopies may obscure the passive detection of smaller, understory trees (Yebra et al. 2018), further limiting the reliability of satellite-derived burn severity metrics in representing fire effects. Post-fire field data such as CBI (Parks et al. 2018a), change in canopy cover, and change in basal area (Miller et al. 2009) can be used to calibrate burn severity indices and derive ecologically meaningful burn severity thresholds, while reducing some uncertainty.

Depending on their magnitude, change estimates are binned into burn severity classes. For our study, we used CBI thresholds (Parks et al. 2014a) to simplify the interpretation of fire effects and quantify the area burned in each class by treatment type. The occurrence of high burn severity caused by pre-Bootleg Rx may have introduced inaccuracy in our post-Bootleg burn severity assessment. Specifically, at the pixel scale, the occurrence of trees already consumed by Rx may have reduced RBR values, inflating estimates of area burned at low or moderate severity. Tree mortality induced by prescribed fire was less than 5% across the study area, and only some patches measuring less than 2 ha had tree mortality greater than 5%, according to the local land manager (C. Bienz, The Nature Conservancy, Oregon, USA, personal communication). Thus, we believe that any possible inaccuracies related to low- and moderate-severity estimates were not substantial and likely had minimal, if any, influence on the results.

Conclusions

Understanding the complex relationships that drive burn severity is critical for informing future land management programs. We investigated fuel reduction prescriptions, including thinning, prescribed fire, and their combination. Our findings indicate that while all treatments mitigated burn severity, those involving prescribed fire were disproportionately more effective. Where fire suppression occurred, we observed a decreasing trend in predicted burn severity within Rx and TxRx units, and more variable effects within Tx units. Furthermore, the occurrence of moist, wetland soils likely contributed to the low burn severity observed within thinning treatments and untreated forests.

Through SHAP analysis, we demonstrated that the local effect of each predictor varied spatially. Under similarly severe weather conditions, the global-impact analysis identified the presence or absence of prescribed fire as the most important driver of predicted burn severity. Furthermore, both the local-effect analysis and burn-severity assessment indicated that prescribed fire alone was as effective as thinning and prescribed fire combined. Critical variables that initially seemed to reflect water-stress conditions and topographic positioning were found to be proxies for fuel structure and accumulation, further underscoring the central role of fuel characteristics in influencing burn severity. These methods allowed us to interpret relationships that would have otherwise been overlooked or potentially misunderstood in an exclusively global analysis, rather than one that considers both global and local perspectives. Additionally, integrating the expertise of local managers with scientific analysis provided the opportunity to conduct a more accurate burn severity assessment and improve our interpretation of the results.

Conclusively, this study contributes to the body of knowledge by providing a reproducible framework to explain the effect of contagious processes like fire at both global and local scales.

It also offers insights to guide and improve fire and fuel management practices across multi-ownership landscapes.

Tables

Table 1: Incident Action Plans fire weather data provided by TNC. FM = fuel moisture. MIN RH = minimum relative humidity. T MAX K = maximum temperature in degrees Kelvin. T MAX = maximum temperature in degrees Celsius. ERC = energy release component. Maximum wind speed exceeded 20 mph on several days, reaching 40 mph on July 18 for a short period of time.

Julian day	July 2021 day	FM 100	FM 1000	MIN RH	T MAX K	T MAX C	ERC
194	13	< 8	< 9	14.5	306.5	33.2	66.0
195	14	< 8	< 9	14.0	307.6	34.3	65.0
196	15	< 8	< 9	12.0	305.4	32.2	68.0
198	17	< 7	< 9	12.0	305.4	32.2	67.0
200	19	< 7	< 9	13.0	303.7	30.6	64.0
201	20	< 7	< 9	13.0	304.3	31.1	64.0
202	21	< 7	< 9	13.0	304.3	31.1	74.0

Table 2: List of predictors included in the final analysis. All topographic variables were calculated applying 15, 45, 135, 270 m windows, except for topographic position index which was calculated applying 200, 500, 1000, 2000, 4000 m windows.

Predictors	Resolution (m)	Unit	Source/software
Management			
Prescribed fire	10	unitless	TNC; IFTDSS
Mechanical thinning	10	unitless	TNC; IFTDSS
Firefighting	10	unitless	Survey
Forest structure			
Canopy cover	30	%	FUSION
Canopy rumple	30	unitless	FUSION
Topography			
Topographic position index	15	unitless	FUSION
Aspect	15	degrees AZ	FUSION
Slope	15	degrees	FUSION
Solar radiation index	15	unitless	FUSION
Weather			
Maximum temperature	4000	Kelvin	Abatzoglou 2013; NIROPS
Northsouthness maximum wind speed	90	cosine transformed radians	WindNinja
Snow cover frequency	500	%	Crumley et al. 2020
Evaporative stress index	70	unitless	Fisher 2018
Climate normal			
Actual Evapotranspiration 1981-2010	90	mm	Cansler et al. 2022 (Appendix B)
Distance to streams and wetlands	10	m	ODSL; ODFW

Figures

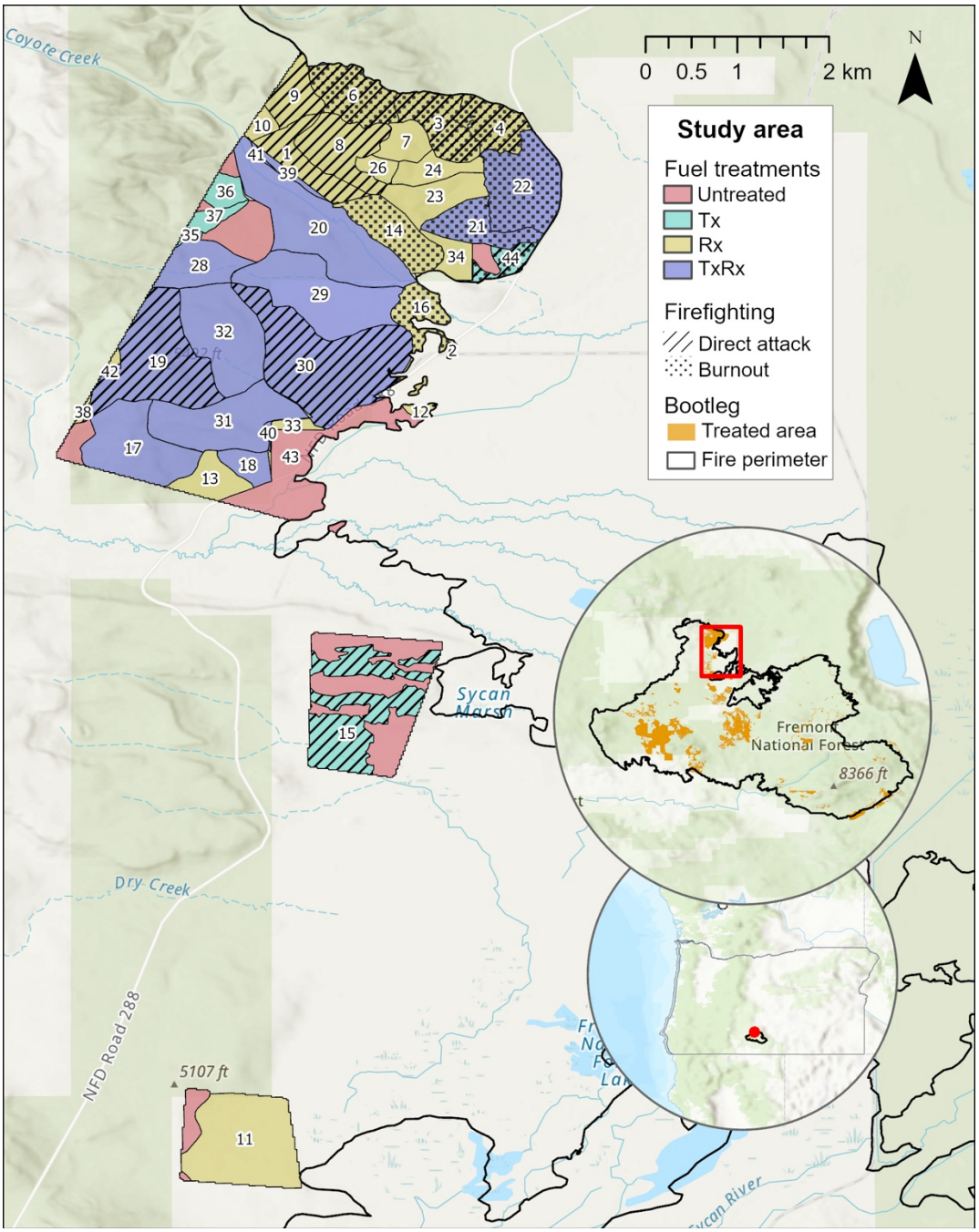

Fig. 1: Map showing the study area footprint, fuel treatments, and firefighting operations. Each individual polygon represents a unit, except for the untreated area, which is characterized by multiple polygons all labeled as unit 43. Embedded overview maps include extent indicators (red rectangle and dot) to show the location of the study area (near Sycan Marsh, south-central Oregon, US) at different scales.

Fig. 2: Photos of fuel treatments and fire tornado effects. A) post-thinning fuel conditions and soil disturbance. B) post-prescribed fire with >5% mortality. C) tree uprooted by a wildfire tornado. D) post prescribed fire fuel conditions with <5% mortality. E) High severity burns in forested riparian area (northeast corner of TxRx unit 20; Coyote Creek; April 25th, 2024). Photos were taken at three different locations within our study area (near Sycan Marsh, south-central Oregon, US). Photo credit: Craig Bienz (TNC; A, B, D); Alina Cansler (C); Astrid Sanna (E).

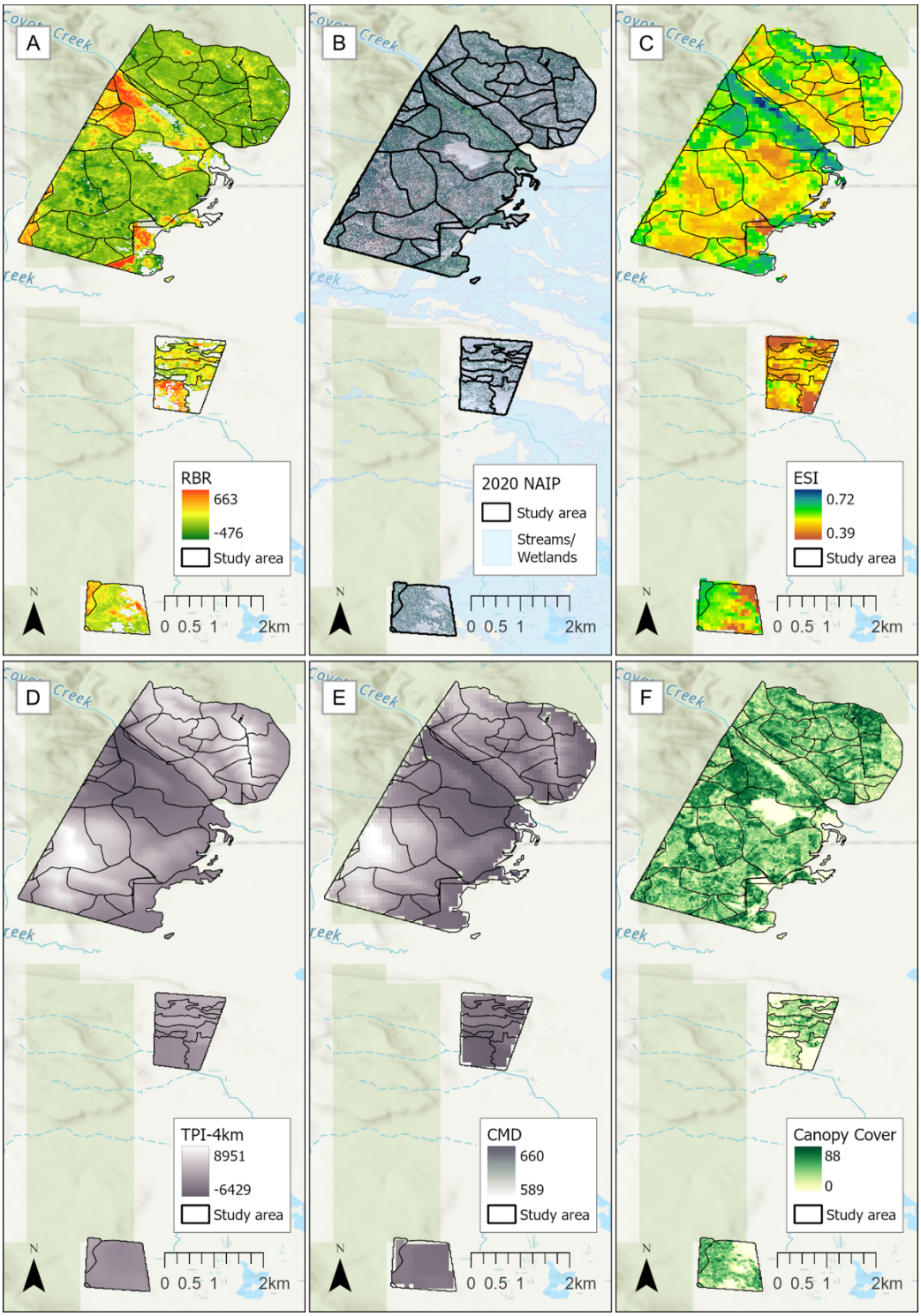

Fig. 3: A) Raster of continuous RBR at 10-m resolution, including only pixels representing canopy cover >10%, and representing one-year post-fire burn severity for the 2021 Bootleg Fire near Sycan Marsh (south-central Oregon, US). B) Map including 2020 NAIP imagery at 0.6-m resolution. The background map shows streams and wetlands cover. C) ESI. D) TPI-4km. E) CMD. F) Canopy cover (above 2 m). Raster layers from B to F show values for entire study area.

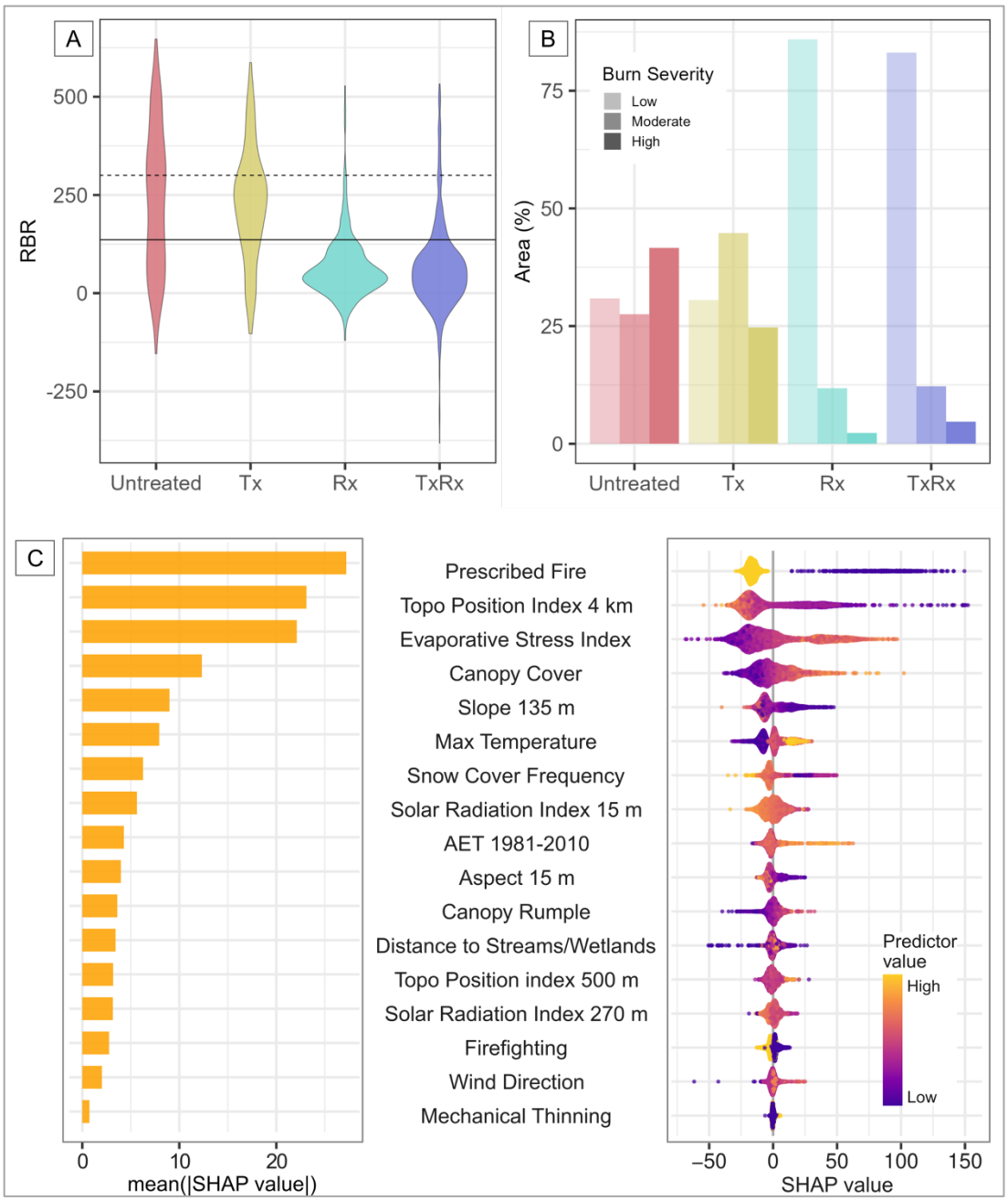

Fig. 4: Graphs supporting the one-year post-fire burn severity analysis for the 2021 Bootleg Fire near Sycan Marsh (south-central Oregon, US). A) RBR distribution by treatment type. Solid and dotted horizontal lines represent low and moderate burn severity thresholds, respectively. B) Percentages of area burned across different severity classes by treatment type. C) SHAP importance plots presenting the global impact (left) and the local effect (right) of each predictor on burn severity in decreasing order of importance. Left plot: x-axis shows the mean of the absolute SHAP values. Right plot: x-axis shows negative and positive SHAP values to indicate a decrease and an increase in predicted burn severity, respectively (relative to the predicted mean). The magnitude of SHAP values reflects the strength of the local effect of each feature value on the prediction, with larger absolute values indicating a greater influence.

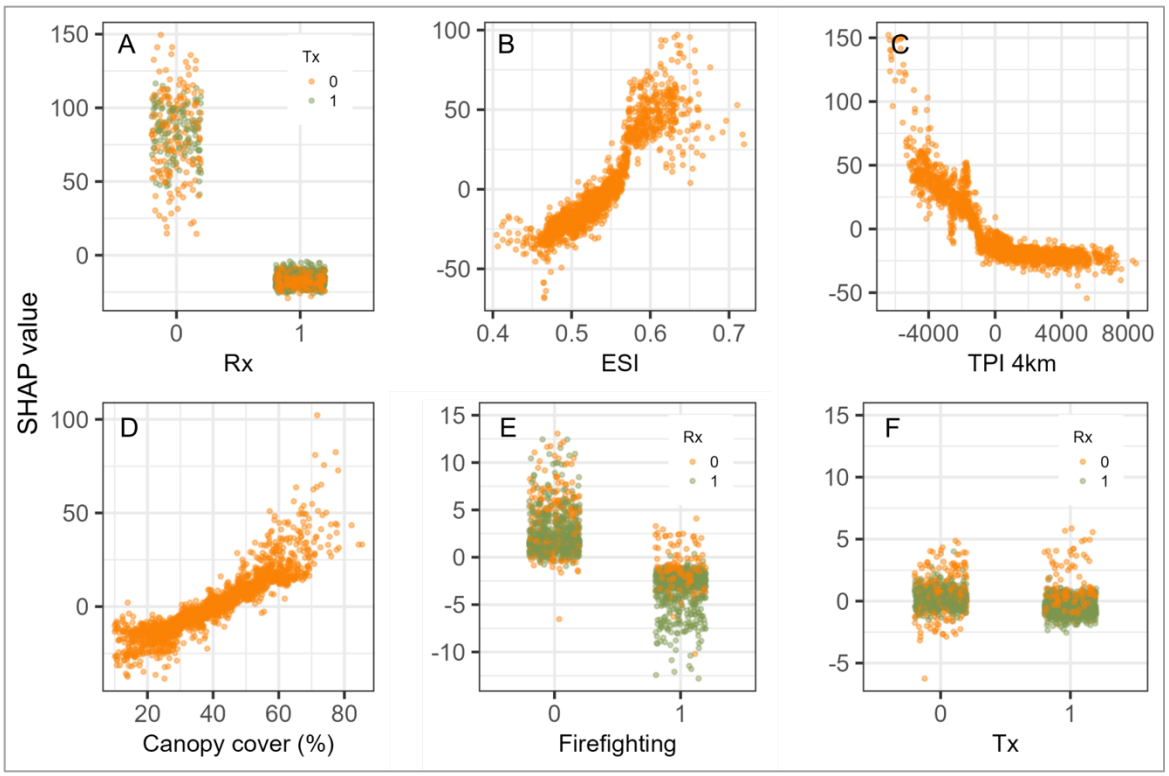

Fig. 5: Scatter plots supporting the one-year post-fire burn severity analysis for the 2021 Bootleg Fire near Sycan Marsh (south-central Oregon, US). Each plot shows important predictors (x-axes) against SHAP values (y-axes). Predictors are presented in order of decreasing importance. Rx (A) is color-coded by Tx values (0 = absent, 1 = present), and untreated observations are represented by Rx = 0 and Tx = 0. Firefighting (E) and Tx (F) are color coded by Rx values (0 = absent, 1 = present). Firefighting operations were conducted only in treated units, thus Firefighting = 1 and Rx = 0 indicate Tx observations subjected to fire suppression, while Firefighting = 0 and Rx = 0 indicate either Tx or untreated observations where fire was not suppressed. In plot F, untreated observations are represented by Tx = 0 and Rx = 0. On the y-axis, negative SHAP values indicate a decrease in the predicted burn severity, while positive SHAP values indicate an increase (relative to the predicted mean). The magnitude of SHAP values reflects the strength of the local effect of each feature value on the prediction, with larger absolute values indicating a greater influence.

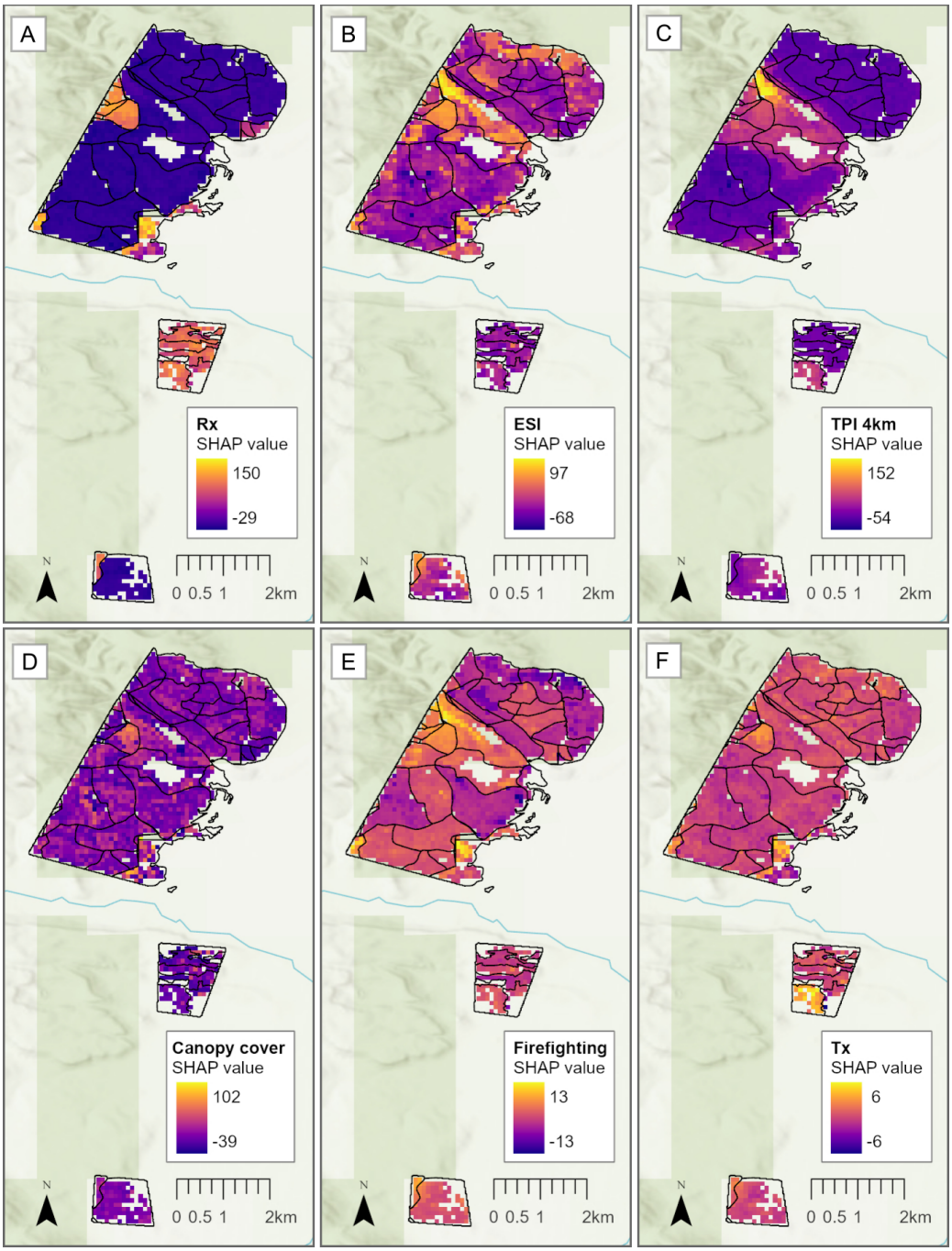

Fig. 6: Maps supporting the one-year post-fire burn severity analysis for the 2021 Bootleg Fire near Sycan Marsh (south-central Oregon, US). Each map represents rasterized SHAP values (90-m) for the top four burn severity drivers (Rx, ESI, TPI-4km, Canopy cover) along with Firefighting and Tx, which are displayed in order of descending importance. Each raster matches the extent of the study area and is overlaid by the fuel treatments layer (black lines). Negative SHAP values indicate a decrease in the predicted burn severity, while positive SHAP values indicate an increase (relative to the predicted mean). The magnitude of SHAP values reflects the strength of the local effect of each feature value on the prediction, with larger absolute values indicating a greater influence.

References

Abatzoglou, John T. 2013. “Development of Gridded Surface Meteorological Data for Ecological Applications and Modelling.” *International Journal of Climatology* 33 (1): 121–31. https://doi.org/10.1002/joc.3413.

Agee, James K. 1993. “Fire Ecology of Pacific Northwest Forests,” 513.

Agee, James K. 2003. “Monitoring Postfire Tree Mortality in Mixed-Conifer Forests of Crater Lake, Oregon, USA.” *Natural Areas Journal* 23 (2): 114–20.

Agee, James K, Berni Bahro, Mark A Finney, Philip N Omi, David B Sapsis, Carl N Skinner, Jan W van Wagtendonk, and C Phillip Weatherspoon. 2000. “The Use of Shaded Fuelbreaks in Landscape ®re Management.” *Forest Ecology and Management*.

Agee, James K., and Carl N. Skinner. 2005. “Basic Principles of Forest Fuel Reduction Treatments.” *Forest Ecology and Management* 211 (1–2): 83–96. https://doi.org/10.1016/j.foreco.2005.01.034.

Allen, CD, M Savage, DA Falk, KF Suckling, TW Swetnam, T Schulke, PB Stacey, P Morgan, M Hoffman, and JT Klingel. 2002. “Ecological Restoration of Southwestern Ponderosa Pine Ecosystems: A Broad Perspective.” *ECOLOGICAL APPLICATIONS* 12 (5): 1418–33.

Andersen, Hans-Erik, Robert J. McGaughey, and Stephen E. Reutebuch. 2005. “Estimating Forest Canopy Fuel Parameters Using LIDAR Data.” *Remote Sensing of Environment* 94 (4): 441–49. https://doi.org/10.1016/j.rse.2004.10.013.

Arno, Stephen F., Michael G. Hartwell, Intermountain Research Station (Ogden, Utah), and Joe H. Scott. 1995. *Age-Class Structure of Old Growth Ponderosa Pine/Douglas-Fir Stands and Its Relationship to Fire History /*. Ogden, UT : U.S. Dept. of Agriculture, Forest Service, Intermountain Research Station,. https://doi.org/10.5962/bhl.title.68858.

Bentz, Barbara. 2008. “Mountain Pine Beetle, Dendroctonus Ponderosae (Coleoptera: Curculionidae, Scolytinae).”

Birch, Donovan S., Penelope Morgan, Crystal A. Kolden, John T. Abatzoglou, Gregory K. Dillon, Andrew T. Hudak, and Alistair M. S. Smith. 2015. “Vegetation, Topography and Daily Weather Influenced Burn Severity in Central Idaho and Western Montana Forests.” *Ecosphere* 6 (1): 1–23. https://doi.org/10.1890/ES14-00213.1.

Breiman, Leo. 2001. *Random Forests*. Vol. 45. https://doi.org/10.1023/A:1010933404324.

Brodie, Emily, Eric E. Knapp, Wesley Brooks, Stacy A. Drury, and Martin W. Ritchie. 2023. “Forest Thinning and Prescribed Burning Treatments Reduce Wildfire Severity and Buffer the Impacts of Severe Fire Weather.” Preprint. In Review. https://doi.org/10.21203/rs.3.rs-3287202/v1.

Cansler, C. Alina, Van R. Kane, Paul F. Hessburg, Jonathan T. Kane, Sean M.A. Jeronimo, James A. Lutz, Nicholas A. Povak, Derek J. Churchill, and Andrew J. Larson. 2022. “Previous Wildfires and Management Treatments Moderate Subsequent Fire Severity.” *Forest Ecology and Management* 504 (January):119764. https://doi.org/10.1016/j.foreco.2021.119764.

Cansler, C. Alina, and Donald McKenzie. 2014. “Climate, Fire Size, and Biophysical Setting Control Fire Severity and Spatial Pattern in the Northern Cascade Range, USA.” *Ecological Applications* 24 (5): 1037–56. https://doi.org/10.1890/13-1077.1.

Churchill, Derek J, Sean MA Jeronimo, Andrew J Larson, Paul Fischer, Matt C Dahlgreen, and Jerry F Franklin. 2016. “The ICO Approach to Quantifying and Restoring Forest Spatial Pattern: Implementation Guide.”

Crumley, Ryan L., Ross T. Palomaki, Anne W. Nolin, Eric A. Sproles, and Eugene J. Mar. 2020. “SnowCloudMetrics: Snow Information for Everyone.” *Remote Sensing* 12 (20): 3341. https://doi.org/10.3390/rs12203341.

Das, Adrian J., Nathan L. Stephenson, and Kristin P. Davis. 2016. “Why Do Trees Die? Characterizing the Drivers of Background Tree Mortality.” *Ecology* 97 (10): 2616–27. https://doi.org/10.1002/ecy.1497.

Davis, Kimberley T., Jamie Peeler, Joseph Fargione, Ryan D. Haugo, Kerry L. Metlen, Marcos D. Robles, and Travis Woolley. 2024. “Tamm Review: A Meta-Analysis of Thinning, Prescribed Fire, and Wildfire Effects on Subsequent Wildfire Severity in Conifer Dominated Forests of the Western US.” *Forest Ecology and Management* 561 (June):121885. https://doi.org/10.1016/j.foreco.2024.121885.

Dillon, Gregory K., Zachary A. Holden, Penelope Morgan, Michael A. Crimmins, Emily K. Heyerdahl, and Charles H. Luce. 2011. “Both Topography and Climate Affected Forest and Woodland Burn Severity in Two Regions of the Western US, 1984 to 2006.” *Ecosphere* 2 (12): art130. https://doi.org/10.1890/ES11-00271.1.

Finney, Mark A, Charles W McHugh, and Isaac C Grenfell. 2005. “Stand- and Landscape-Level Effects of Prescribed Burning on Two Arizona Wildfires.” *Canadian Journal of Forest Research* 35 (7): 1714–22. https://doi.org/10.1139/x05-090.

Fisher, Joshua B. 2018. “Level-4 Evaporative Stress Index.”

Forthofer, Jason M. 2007. “Modeling Wind in Complex Terrain for Use in Fire Spread Prediction.” Colorado State University. https://www.firelab.org/sites/default/files/2021-04/Forthofer_2007_thesis.pdf.

Fountain, Henry. 2021. “How Bad Is the Bootleg Fire? It’s Generating Its Own Weather.” *The New York Times*, 2021.

Fry, Danny L., and Scott L. Stephens. 2006. “Influence of Humans and Climate on the Fire History of a Ponderosa Pine-Mixed Conifer Forest in the Southeastern Klamath Mountains, California.” *Forest Ecology and Management* 223 (1–3): 428–38. https://doi.org/10.1016/j.foreco.2005.12.021.

Fulé, Peter Z., Joseph E. Crouse, John Paul Roccaforte, and Elizabeth L. Kalies. 2012. “Do Thinning and/or Burning Treatments in Western USA Ponderosa or Jeffrey Pine-Dominated Forests Help Restore Natural Fire Behavior?” *Forest Ecology and Management* 269 (April):68–81. https://doi.org/10.1016/j.foreco.2011.12.025.

Furniss, Tucker J., Van R. Kane, Andrew J. Larson, and James A. Lutz. 2020. “Detecting Tree Mortality with Landsat-Derived Spectral Indices: Improving Ecological Accuracy by Examining Uncertainty.” *Remote Sensing of Environment* 237 (February):111497. https://doi.org/10.1016/j.rse.2019.111497.

Giglio, Louis, Tatiana Loboda, David P. Roy, Brad Quayle, and Christopher O. Justice. 2009. “An Active-Fire Based Burned Area Mapping Algorithm for the MODIS Sensor.” *Remote Sensing of Environment* 113 (2): 408–20. https://doi.org/10.1016/j.rse.2008.10.006.

Gorelick, Noel, Matt Hancher, Mike Dixon, Simon Ilyushchenko, David Thau, and Rebecca Moore. 2017. “Google Earth Engine: Planetary-Scale Geospatial Analysis for Everyone.”

Remote Sensing of Environment 202 (December):18–27. https://doi.org/10.1016/j.rse.2017.06.031.

Hagmann, R. K., P. F. Hessburg, S. J. Prichard, N. A. Povak, P. M. Brown, P. Z. Fulé, R. E. Keane, et al. 2021. "Evidence for Widespread Changes in the Structure, Composition, and Fire Regimes of Western North American Forests." *Ecological Applications* 31 (8): e02431. https://doi.org/10.1002/eap.2431.

Hagmann, R. Keala, Jerry F. Franklin, and K. Norman Johnson. 2013. "Historical Structure and Composition of Ponderosa Pine and Mixed-Conifer Forests in South-Central Oregon." *Forest Ecology and Management* 304 (September):492–504. https://doi.org/10.1016/j.foreco.2013.04.005.

Hagmann, R. Keala, Andrew G. Merschel, and Matthew J. Reilly. 2019. "Historical Patterns of Fire Severity and Forest Structure and Composition in a Landscape Structured by Frequent Large Fires: Pumice Plateau Ecoregion, Oregon, USA." *Landscape Ecology* 34 (3): 551–68. https://doi.org/10.1007/s10980-019-00791-1.

Hagmann, R.K., P.F. Hessburg, R.B. Salter, A.G. Merschel, and M.J. Reilly. 2022. "Contemporary Wildfires Further Degrade Resistance and Resilience of Fire-Excluded Forests." *Forest Ecology and Management* 506 (February):119975. https://doi.org/10.1016/j.foreco.2021.119975.

Halofsky, JE, DL Peterson, and BJ Harvey. 2020. "Changing Wildfire, Changing Forests: The Effects of Climate Change on Fire Regimes and Vegetation in the Pacific Northwest, USA." *FIRE ECOLOGY* 16 (1). https://doi.org/10.1186/s42408-019-0062-8.

Hanan, EJ, JN Ren, CL Tague, CA Kolden, JT Abatzoglou, RR Bart, MC Kennedy, ML Liu, and JC Adam. 2021. "How Climate Change and Fire Exclusion Drive Wildfire Regimes at Actionable Scales." *ENVIRONMENTAL RESEARCH LETTERS* 16 (2). https://doi.org/10.1088/1748-9326/abd78e.

Harbert, Steve, Andrew Hudak, Research Forester, Laura Mayer, Tim Rich, and Sarah Robertson. 2007. "Pacific Northwest Region, USDA Forest Service Oregon State Office, USDI Bureau of Land Management."

Hargreaves, George H., and Richard G. Allen. 2003. "History and Evaluation of Hargreaves Evapotranspiration Equation." *Journal of Irrigation and Drainage Engineering* 129 (1): 53–63. https://doi.org/10.1061/(ASCE)0733-9437(2003)129:1(53).

Harris, Lucas B., Stacy A. Drury, Calvin A. Farris, and Alan H. Taylor. 2021. "Prescribed Fire and Fire Suppression Operations Influence Wildfire Severity under Severe Weather in Lassen Volcanic National Park, California, USA." *International Journal of Wildland Fire* 30 (7): 536–51. https://doi.org/10.1071/WF20163.

Harris, Lucas, and Alan H. Taylor. 2017. "Previous Burns and Topography Limit and Reinforce Fire Severity in a Large Wildfire." *Ecosphere* 8 (11). https://doi.org/10.1002/ecs2.2019.

Haugo, Ryan D., Bryce S. Kellogg, C. Alina Cansler, Crystal A. Kolden, Kerry B. Kemp, James C. Robertson, Kerry L. Metlen, Nicole M. Vaillant, and Christina M. Restaino. 2019. "The Missing Fire: Quantifying Human Exclusion of Wildfire in Pacific Northwest Forests, USA." *Ecosphere* 10 (4): e02702. https://doi.org/10.1002/ecs2.2702.

Hessburg, Paul F., Carol L. Miller, Sean A. Parks, Nicholas A. Povak, Alan H. Taylor, Philip E. Higuera, Susan J. Prichard, et al. 2019. "Climate, Environment, and Disturbance History Govern Resilience of Western North American Forests." *Frontiers in Ecology and Evolution* 7 (July):239. https://doi.org/10.3389/fevo.2019.00239.

Holland, Timothy G., Samuel G. Evans, Jonathan W. Long, Charles Maxwell, Robert M. Scheller, and Matthew D. Potts. 2022. "The Management Costs of Alternative Forest Management Strategies in the Lake Tahoe Basin." *Ecology and Society* 27 (4). https://doi.org/10.5751/ES-13481-270443.

Hood, Sharon M., Sheri L. Smith, and Daniel R. Cluck. 2010. "Predicting Mortality for Five California Conifers Following Wildfire." *Forest Ecology and Management* 260 (5): 750–62. https://doi.org/10.1016/j.foreco.2010.05.033.

Hood, Sharon M, J Morgan Varner, Phillip Van Mantgem, and C Alina Cansler. 2018. "Fire and Tree Death: Understanding and Improving Modeling of Fire-Induced Tree Mortality." *Environmental Research Letters* 13 (11): 113004. https://doi.org/10.1088/1748-9326/aae934.

Howe, Alexander A., Sean A. Parks, Brian J. Harvey, Saba J. Saberi, James A. Lutz, and Larissa L. Yocom. 2022. "Comparing Sentinel-2 and Landsat 8 for Burn Severity Mapping in Western North America." *Remote Sensing* 14 (20): 5249. https://doi.org/10.3390/rs14205249.

Hudak, Andrew T., Ian Rickert, Penelope Morgan, Eva Strand, Sarah A. Lewis, Peter R. Robichaud, Chad Hoffman, and Zachary A. Holden. 2011. "Review of Fuel Treatment Effectiveness in Forests and Rangelands and a Case Study from the 2007 Megafires in Central, Idaho, USA." RMRS-GTR-252. Ft. Collins, CO: U.S. Department of Agriculture, Forest Service, Rocky Mountain Research Station. https://doi.org/10.2737/RMRS-GTR-252.

IFTDSS. 2021. "Interagency Fuel Treatment Decision Support System." Interagency Fuel Treatment Decision Support System. 2021. https://iftdss.firenet.gov.

Johnstone, Jill F, Craig D Allen, Jerry F Franklin, Lee E Frelich, Brian J Harvey, Philip E Higuera, Michelle C Mack, et al. 2016. "Changing Disturbance Regimes, Ecological Memory, and Forest Resilience." *Frontiers in Ecology and the Environment* 14 (7): 369–78. https://doi.org/10.1002/fee.1311.

Kalies, Elizabeth L., and Larissa L. Yocom Kent. 2016. "Tamm Review: Are Fuel Treatments Effective at Achieving Ecological and Social Objectives? A Systematic Review." *Forest Ecology and Management* 375 (September):84–95. https://doi.org/10.1016/j.foreco.2016.05.021.

Kane, Jeffrey M. 2021. "Stand Conditions Alter Seasonal Microclimate and Dead Fuel Moisture in a Northwestern California Oak Woodland." *Agricultural and Forest Meteorology* 308–309 (October):108602. https://doi.org/10.1016/j.agrformet.2021.108602.

Kane, Jeffrey M., J. Morgan Varner, Margaret R. Metz, and Phillip J. Van Mantgem. 2017. "Characterizing Interactions between Fire and Other Disturbances and Their Impacts on Tree Mortality in Western U.S. Forests." *Forest Ecology and Management* 405 (December):188–99. https://doi.org/10.1016/j.foreco.2017.09.037.

Kane, Van R., C. Alina Cansler, Nicholas A. Povak, Jonathan T. Kane, Robert J. McGaughey, James A. Lutz, Derek J. Churchill, and Malcolm P. North. 2015. "Mixed Severity Fire Effects within the Rim Fire: Relative Importance of Local Climate, Fire Weather, Topography, and Forest Structure." *Forest Ecology and Management* 358 (December):62–79. https://doi.org/10.1016/j.foreco.2015.09.001.

Kane, Van R., James A. Lutz, C. Alina Cansler, Nicholas A. Povak, Derek J. Churchill, Douglas F. Smith, Jonathan T. Kane, and Malcolm P. North. 2015. "Water Balance and

Topography Predict Fire and Forest Structure Patterns." *Forest Ecology and Management* 338 (February):1–13. https://doi.org/10.1016/j.foreco.2014.10.038.
Kelsey, Rick G, and Gladwin Joseph. 2003. "Ethanol in Ponderosa Pine as an Indicator of Physiological Injury from Fire and Its Relationship to Secondary Beetles." *Canadian Journal of Forest Research* 33 (5): 870–84. https://doi.org/10.1139/x03-007.
Key, Carl H, and Nathan C Benson. 2006. "Landscape Assessment (LA)," 55.
Knapp, Eric E., Jamie M. Lydersen, Malcolm P. North, and Brandon M. Collins. 2017. "Efficacy of Variable Density Thinning and Prescribed Fire for Restoring Forest Heterogeneity to Mixed-Conifer Forest in the Central Sierra Nevada, CA." *Forest Ecology and Management* 406 (December):228–41. https://doi.org/10.1016/j.foreco.2017.08.028.
Kuhn, Max. 2008. "Building Predictive Models in R Using the Caret Package." *Journal of Statistical Software* 28 (November):1–26. https://doi.org/10.18637/jss.v028.i05.
Larson, Andrew J., R. Travis Belote, C. Alina Cansler, Sean A. Parks, and Matthew S. Dietz. 2013. "Latent Resilience in Ponderosa Pine Forest: Effects of Resumed Frequent Fire." *Ecological Applications* 23 (6): 1243–49. https://doi.org/10.1890/13-0066.1.
Lundberg, Scott M., Gabriel G. Erion, and Su-In Lee. 2019. "Consistent Individualized Feature Attribution for Tree Ensembles." arXiv. http://arxiv.org/abs/1802.03888.
Lundberg, Scott M, and Su-In Lee. 2017. "A Unified Approach to Interpreting Model Predictions."
Lutz, James A., Tucker J. Furniss, Daniel J. Johnson, Stuart J. Davies, David Allen, Alfonso Alonso, Kristina J. Anderson-Teixeira, et al. 2018. "Global Importance of Large-diameter Trees." *Global Ecology and Biogeography* 27 (7): 849–64. https://doi.org/10.1111/geb.12747.
Ma, Siyan, Amy Concilio, Brian Oakley, Malcolm North, and Jiquan Chen. 2010. "Spatial Variability in Microclimate in a Mixed-Conifer Forest before and after Thinning and Burning Treatments." *Forest Ecology and Management* 259 (5): 904–15. https://doi.org/10.1016/j.foreco.2009.11.030.
Maksymiuk, Szymon, Alicja Gosiewska, and Przemyslaw Biecek. 2021. "Landscape of R Packages for eXplainable Artificial Intelligence." arXiv. http://arxiv.org/abs/2009.13248.
McGaughey, Robert J. 2020. "FUSION/LDV: Software for LIDAR Data Analysis and Visualization." 2020. http://forsys.cfr.washington.edu/software/fusion/FUSION_manual.pdf.
Miller, Carol, and Dean L. Urban. 2000. "Modeling the Effects of Fire Management Alternatives on Sierra Nevada Mixed-Conifer Forests." *Ecological Applications* 10 (1): 85–94. https://doi.org/10.2307/2640988.
Miller, Jay D., Eric E. Knapp, Carl H. Key, Carl N. Skinner, Clint J. Isbell, R. Max Creasy, and Joseph W. Sherlock. 2009. "Calibration and Validation of the Relative Differenced Normalized Burn Ratio (RdNBR) to Three Measures of Fire Severity in the Sierra Nevada and Klamath Mountains, California, USA." *Remote Sensing of Environment* 113 (3): 645–56. https://doi.org/10.1016/j.rse.2008.11.009.
Miller, Jay D., Hugh D. Safford, and Kevin R. Welch. 2016. "Using One Year Post-Fire Fire Severity Assessments to Estimate Longer-Term Effects of Fire in Conifer Forests of Northern and Eastern California, USA." *Forest Ecology and Management* 382 (December):168–83. https://doi.org/10.1016/j.foreco.2016.10.017.

Moghaddas, Jason J., and Larry Craggs. 2007. “A Fuel Treatment Reduces Fire Severity and Increases Suppression Efficiency in a Mixed Conifer Forest.” *International Journal of Wildland Fire* 16 (6): 673. https://doi.org/10.1071/WF06066.

Molnar, Christoph. 2023. *Interpretable Machine Learning. A Guide for Making Black Box Models Explainable*. Second. https://christophm.github.io/interpretable-ml-book/index.html.

Murphy, Kate, Tim Rich, and Tim Sexton. 2007. “An Assessment of Fuel Treatment Effects on Fire Behavior, Suppression Effectiveness, and Structure Ignition on the Angora Fire.” R5-TP-025. USDA Forest Service. https://www.tahoelivingwithfire.com/wp-content/uploads/2018/11/murphy_usfs_2007_a.pdf.

Naimi, Babak, Nicholas A. S. Hamm, Thomas A. Groen, Andrew K. Skidmore, Albertus G. Toxopeus, and Sara Alibakhshi. 2019. “ELSA: Entropy-Based Local Indicator of Spatial Association.” *Spatial Statistics* 29 (March):66–88. https://doi.org/10.1016/j.spasta.2018.10.001.

North, Malcolm P., Ryan E. Tompkins, Alexis A. Bernal, Brandon M. Collins, Scott L. Stephens, and Robert A. York. 2022. “Operational Resilience in Western US Frequent-Fire Forests.” *Forest Ecology and Management* 507 (March):120004. https://doi.org/10.1016/j.foreco.2021.120004.

ODFW. 2021. “Oregon Hydrography Whole Stream Routes.” 2021. https://nrimp.dfw.state.or.us/DataClearinghouse/default.aspx?p=202&XMLname=1124.xml.

ODSL. 2021. “Statewide Wetlands Inventory.” 2021. https://maps.dsl.state.or.us/swi/.

Parker, Geoffrey G., Mark E. Harmon, Michael A. Lefsky, Jiquan Chen, Robert Van Pelt, Stuart B. Weis, Sean C. Thomas, William E. Winner, David C. Shaw, and Jerry F. Frankling. 2004. “Three-Dimensional Structure of an Old-Growth Pseudotsuga-Tsuga Canopy and Its Implications for Radiation Balance, Microclimate, and Gas Exchange.” *Ecosystems* 7 (5). https://doi.org/10.1007/s10021-004-0136-5.

Parker, Thomas J., Karen M. Clancy, and Robert L. Mathiasen. 2006. “Interactions among Fire, Insects and Pathogens in Coniferous Forests of the Interior Western United States and Canada.” *Agricultural and Forest Entomology* 8 (3): 167–89. https://doi.org/10.1111/j.1461-9563.2006.00305.x.

Parks, Sean A., Lisa M. Holsinger, Kori Blankenship, Gregory K. Dillon, Sara A. Goeking, and Randy Swaty. 2023. “Contemporary Wildfires Are More Severe Compared to the Historical Reference Period in Western US Dry Conifer Forests.” *Forest Ecology and Management* 544 (September):121232. https://doi.org/10.1016/j.foreco.2023.121232.

Parks, Sean A., Lisa M. Holsinger, Carol Miller, and Cara R. Nelson. 2015. “Wildland Fire as a Self-Regulating Mechanism: The Role of Previous Burns and Weather in Limiting Fire Progression.” *Ecological Applications* 25 (6): 1478–92. https://doi.org/10.1890/14-1430.1.

Parks, Sean A, Lisa M Holsinger, Matthew H Panunto, W Matt Jolly, Solomon Z Dobrowski, and Gregory K Dillon. 2018. “High-Severity Fire: Evaluating Its Key Drivers and Mapping Its Probability across Western US Forests.” *Environmental Research Letters* 13 (4): 044037. https://doi.org/10.1088/1748-9326/aab791.

Parks, Sean A., Carol Miller, Cara R. Nelson, and Zachary A. Holden. 2014. “Previous Fires Moderate Burn Severity of Subsequent Wildland Fires in Two Large Western US

Wilderness Areas." *Ecosystems. 17: 29-42.*, 29–42. https://doi.org/10.1007/s10021-013-9704-x.
Parks, Sean A., Carol Miller, Marc-André Parisien, Lisa M. Holsinger, Solomon Z. Dobrowski, and John Abatzoglou. 2015. "Wildland Fire Deficit and Surplus in the Western United States, 1984–2012." *Ecosphere* 6 (12): 1–13. https://doi.org/10.1890/ES15-00294.1.
Parks, Sean, Gregory Dillon, and Carol Miller. 2014. "A New Metric for Quantifying Burn Severity: The Relativized Burn Ratio." *Remote Sensing* 6 (3): 1827–44. https://doi.org/10.3390/rs6031827.
Parks, Sean, Lisa Holsinger, Morgan Voss, Rachel Loehman, and Nathaniel Robinson. 2018. "Mean Composite Fire Severity Metrics Computed with Google Earth Engine Offer Improved Accuracy and Expanded Mapping Potential." *Remote Sensing* 10 (6): 879. https://doi.org/10.3390/rs10060879.
Picchio, Rodolfo, Piotr S. Mederski, and Farzam Tavankar. 2020. "How and How Much, Do Harvesting Activities Affect Forest Soil, Regeneration and Stands?" *Current Forestry Reports* 6 (2): 115–28. https://doi.org/10.1007/s40725-020-00113-8.
Povak, Nicholas A., Van R. Kane, Brandon M. Collins, Jamie M. Lydersen, and Jonathan T. Kane. 2020. "Multi-Scaled Drivers of Severity Patterns Vary across Land Ownerships for the 2013 Rim Fire, California." *Landscape Ecology* 35 (2): 293–318. https://doi.org/10.1007/s10980-019-00947-z.
Prichard, Susan J., Paul F. Hessburg, R. Keala Hagmann, Nicholas A. Povak, Solomon Z. Dobrowski, Matthew D. Hurteau, Van R. Kane, et al. 2021. "Adapting Western North American Forests to Climate Change and Wildfires: 10 Common Questions." *Ecological Applications* 31 (8): e02433. https://doi.org/10.1002/eap.2433.
Prichard, Susan J., and Maureen C. Kennedy. 2014. "Fuel Treatments and Landform Modify Landscape Patterns of Burn Severity in an Extreme Fire Event." *Ecological Applications* 24 (3): 571–90. https://doi.org/10.1890/13-0343.1.
Prichard, Susan J., Nicholas A. Povak, Maureen C. Kennedy, and David W. Peterson. 2020. "Fuel Treatment Effectiveness in the Context of Landform, Vegetation, and Large, Wind-driven Wildfires." *Ecological Applications* 30 (5): e02104. https://doi.org/10.1002/eap.2104.
Reinhardt, Elizabeth D., Robert E. Keane, David E. Calkin, and Jack D. Cohen. 2008. "Objectives and Considerations for Wildland Fuel Treatment in Forested Ecosystems of the Interior Western United States." *Forest Ecology and Management* 256 (12): 1997–2006. https://doi.org/10.1016/j.foreco.2008.09.016.
Ritchie, Martin W., Carl N. Skinner, and Todd A. Hamilton. 2007. "Probability of Tree Survival after Wildfire in an Interior Pine Forest of Northern California: Effects of Thinning and Prescribed Fire." *Forest Ecology and Management* 247 (1–3): 200–208. https://doi.org/10.1016/j.foreco.2007.04.044.
Rogers, Gene, Wendel Hann, Charley Martin, Tessa Nicolette, and Morgan Pence. 2008. "Fuel Treatment Effects on Fire Behavior, Suppression Effectiveness, and Structure Ignition Grass Valley Fire." R5-TP-026a. https://www.fs.usda.gov/Internet/FSE_DOCUMENTS/fsbdev3_045471.pdf.
RStudio Team. 2020. "RStudio." 2020. http://www.rstudio.com.
Ryan, Kevin C, Eric E Knapp, and J Morgan Varner. 2013. "Prescribed Fire in North American Forests and Woodlands: History, Current Practice, and Challenges." *Frontiers in Ecology and the Environment* 11 (s1). https://doi.org/10.1890/120329.

Ryan, Kevin C., and Tonja S. Opperman. 2013. "LANDFIRE – A National Vegetation/Fuels Data Base for Use in Fuels Treatment, Restoration, and Suppression Planning." *Forest Ecology and Management* 294 (April):208–16. https://doi.org/10.1016/j.foreco.2012.11.003.

Safford, H.D., J.T. Stevens, K. Merriam, M.D. Meyer, and A.M. Latimer. 2012. "Fuel Treatment Effectiveness in California Yellow Pine and Mixed Conifer Forests." *Forest Ecology and Management* 274 (June):17–28. https://doi.org/10.1016/j.foreco.2012.02.013.

Safford, Hugh D., David A. Schmidt, and Chris H. Carlson. 2009. "Effects of Fuel Treatments on Fire Severity in an Area of Wildland–Urban Interface, Angora Fire, Lake Tahoe Basin, California." *Forest Ecology and Management* 258 (5): 773–87. https://doi.org/10.1016/j.foreco.2009.05.024.

Schoennagel, Tania, Thomas T. Veblen, José F. Negron, and Jeremy M. Smith. 2012. "Effects of Mountain Pine Beetle on Fuels and Expected Fire Behavior in Lodgepole Pine Forests, Colorado, USA." Edited by Han Y. H. Chen. *PLoS ONE* 7 (1): e30002. https://doi.org/10.1371/journal.pone.0030002.

Stevens, Jens T., Matthew M. Kling, Dylan W. Schwilk, J. Morgan Varner, and Jeffrey M. Kane. 2020. "Biogeography of Fire Regimes in Western U.S. Conifer Forests: A Trait-based Approach." Edited by Thomas Gillespie. *Global Ecology and Biogeography* 29 (5): 944–55. https://doi.org/10.1111/geb.13079.

Stone, Katharine R., David S. Pilliod, Kathleen A. Dwire, Charles C. Rhoades, Sherry P. Wollrab, and Michael K. Young. 2010. "Fuel Reduction Management Practices in Riparian Areas of the Western USA." *Environmental Management* 46 (1): 91–100. https://doi.org/10.1007/s00267-010-9501-7.

Urza, Alexandra K., Brice B. Hanberry, and Theresa B. Jain. 2023. "Landscape-Scale Fuel Treatment Effectiveness: Lessons Learned from Wildland Fire Case Studies in Forests of the Western United States and Great Lakes Region." *Fire Ecology* 19 (1): 1. https://doi.org/10.1186/s42408-022-00159-y.

USDA. 2021. "NIROPS." 2021. https://fsapps.nwcg.gov/nirops/pages/about.

USGS LiDAR. 2021. "OR_SouthwestCentralSycan_2021_B21." 2021. https://rockyweb.usgs.gov/vdelivery/Datasets/Staged/Elevation/LPC/Projects/OR_SouthwestCentralSycan_2021_B21.

Vaillant, Nicole M., Jo Ann Fites-Kaufman, and Scott L. Stephens. 2006. "Effectiveness of Prescribed Fire as a Fuel Treatment in Californian Coniferous Forests." *International Journal of Wildland Fire* 18 (2): 165. https://doi.org/10.1071/WF06065.

Vaillant, Nicole M., and Elizabeth D. Reinhardt. 2017. "An Evaluation of the Forest Service Hazardous Fuels Treatment Program—Are We Treating Enough to Promote Resiliency or Reduce Hazard?" *Journal of Forestry* 115 (4): 300–308. https://doi.org/10.5849/jof.16-067.

Van Mantgem, Phillip J., Donald A. Falk, Emma C. Williams, Adrian J. Das, and Nathan L. Stephenson. 2018. "Pre-fire Drought and Competition Mediate Post-fire Conifer Mortality in Western U.S. National Parks." *Ecological Applications* 28 (7): 1730–39. https://doi.org/10.1002/eap.1778.

Van Mantgem, Phillip J., Jonathan C. B. Nesmith, MaryBeth Keifer, Eric E. Knapp, Alan Flint, and Lorriane Flint. 2013. "Climatic Stress Increases Forest Fire Severity across the Western U Nited S Tates." Edited by Josep Penuelas. *Ecology Letters* 16 (9): 1151–56. https://doi.org/10.1111/ele.12151.

Van Wagtendonk, Jan W. 2007. “The History and Evolution of Wildland Fire Use.” *Fire Ecology* 3 (2): 3–17. https://doi.org/10.4996/fireecology.0302003.
Wallace Covington, William. 2000. “Helping Western Forests Heal.” *Nature* 408 (6809): 135–36. https://doi.org/10.1038/35041641.
Wang, Tongli, Hamann Andreas, Spittlehouse Dave, and Carroll Carlos. 2023. “ClimateNA.” 2023. https://climatena.ca.
Wang, Tongli, Andreas Hamann, Dave Spittlehouse, and Carlos Carroll. 2016. “Locally Downscaled and Spatially Customizable Climate Data for Historical and Future Periods for North America.” Edited by Inés Álvarez. *PLOS ONE* 11 (6): e0156720. https://doi.org/10.1371/journal.pone.0156720.
Whitehead, Roger J. 2008. *Effect of Commercial Thinning on Within-Stand Microclimate and Fine Fuel Moisture Conditions in a Mature Lodgepole Pine Stand in Southeastern British Columbia*. Victoria, B.C.: Canadian Wood Fibre Centre.
Wright, Marvin N., and Andreas Ziegler. 2017. “Ranger: A Fast Implementation of Random Forests for High Dimensional Data in C++ and R.” *Journal of Statistical Software* 77 (March):1–17. https://doi.org/10.18637/jss.v077.i01.
Yang, Jilei. 2022. “Fast TreeSHAP: Accelerating SHAP Value Computation for Trees.” arXiv. http://arxiv.org/abs/2109.09847.
Yebra, Marta, Xingwen Quan, David Riaño, Pablo Rozas Larraondo, Albert I.J.M. Van Dijk, and Geoffrey J. Cary. 2018. “A Fuel Moisture Content and Flammability Monitoring Methodology for Continental Australia Based on Optical Remote Sensing.” *Remote Sensing of Environment* 212 (June):260–72. https://doi.org/10.1016/j.rse.2018.04.053.
Yocom Kent, Larissa L., Kristen L. Shive, Barbara A. Strom, Carolyn H. Sieg, Molly E. Hunter, Camille S. Stevens-Rumann, and Peter Z. Fulé. 2015. “Interactions of Fuel Treatments, Wildfire Severity, and Carbon Dynamics in Dry Conifer Forests.” *Forest Ecology and Management* 349 (August):66–72. https://doi.org/10.1016/j.foreco.2015.04.004.

Appendix

Tables

Table S1: Comprehensive list of rasterized predictors included in the initial data frame. All topographic variables were calculated applying 15-, 45-, 135-, 270-m windows, except for topographic position index which was calculated applying 200-, 500-, 1000-, 2000-, 4000-m windows. The reduced list of predictors used in the analysis are shown with a *.

Predictors	Resolution (m)	Unit	Source/software
Management			
Prescribed fire *	10	unitless	TNC; IFTDSS
Mechanical thinning *	10	unitless	TNC; IFTDSS
Firefighting *	10	unitless	Survey
Forest structure			
Canopy cover *	30	%	FUSION
Mean canopy height	30	m	FUSION
Canopy base height	30	m	FUSION
Dominant canopy height	30	m	FUSION
Standard deviation canopy height	30	m	FUSION
Canopy rumple *	30	unitless	FUSION
LICO metrics			
Canopy core gap	30	%	NA
1-tree clump canopy	30	%	NA
2to4-tree clump canopy	30	%	NA
5to9-tree clump canopy	30	%	NA
10plus-tree clump canopy	30	%	NA
Topography			
Aspect *	15	degrees AZ	FUSION
Elevation	15	m	FUSION
Curvature	15	unitless	FUSION
Plan curvature	15	unitless	FUSION
Profile curvature	15	unitless	FUSION
Slope *	15	degrees	FUSION
Solar radiation index *	15	unitless	FUSION
Topographic position index *	15	unitless	FUSION
Weather			
Energy release component	4 km	NFDRS fire danger index	Abatzoglou 2013; NIROPS

Fuel moisture (100 and 1000 h)	4 km	%	Abatzoglou 2013; NIROPS
Vapor pressure deficit	4 km	%	Abatzoglou 2013; NIROPS
Maximum temperature *	4 km	Kelvin	Abatzoglou 2013; NIROPS
Minimum relative humidity	4 km	%	Abatzoglou 2013; NIROPS
Maximum wind speed	90 m	mph	WindNinja
Eastwestness maximum wind speed	90 m	sine transformed radians	WindNinja
Northsouthness maximum wind speed *	90 m	cosine transformed radians	WindNinja
Snow cover frequency *	500	%	Crumley et al. 2020
Snow disappearance date	500	Julian days	Crumley et al. 2020
Evaporative stress index *	70	unitless	Fisher 2018
Climate normal			
Actual Evapotranspiration 1981-2010 *	90	mm	Cansler et al. 2022 (Appendix B)
Water deficit 1981-2010	90	mm	Cansler et al. 2022 (Appendix B)
Hargreaves climatic moisture deficit 1991-2020	90	mm	Wang et al. 2016
Mean annual precipitation 1991-2020	90	mm	Wang et al. 2016
May-September precipitation 1991-2020	90	mm	Wang et al. 2016
Precipitation as snow 1991-2020	90	mm	Wang et al. 2016
Existing Vegetation Type 2020	30	unitless	LANDFIRE
Distance to streams and wetlands *	10	m	ODSL; ODFW
Fire Resistance Score	250	unitless	Stevens et al. 2020

Figures

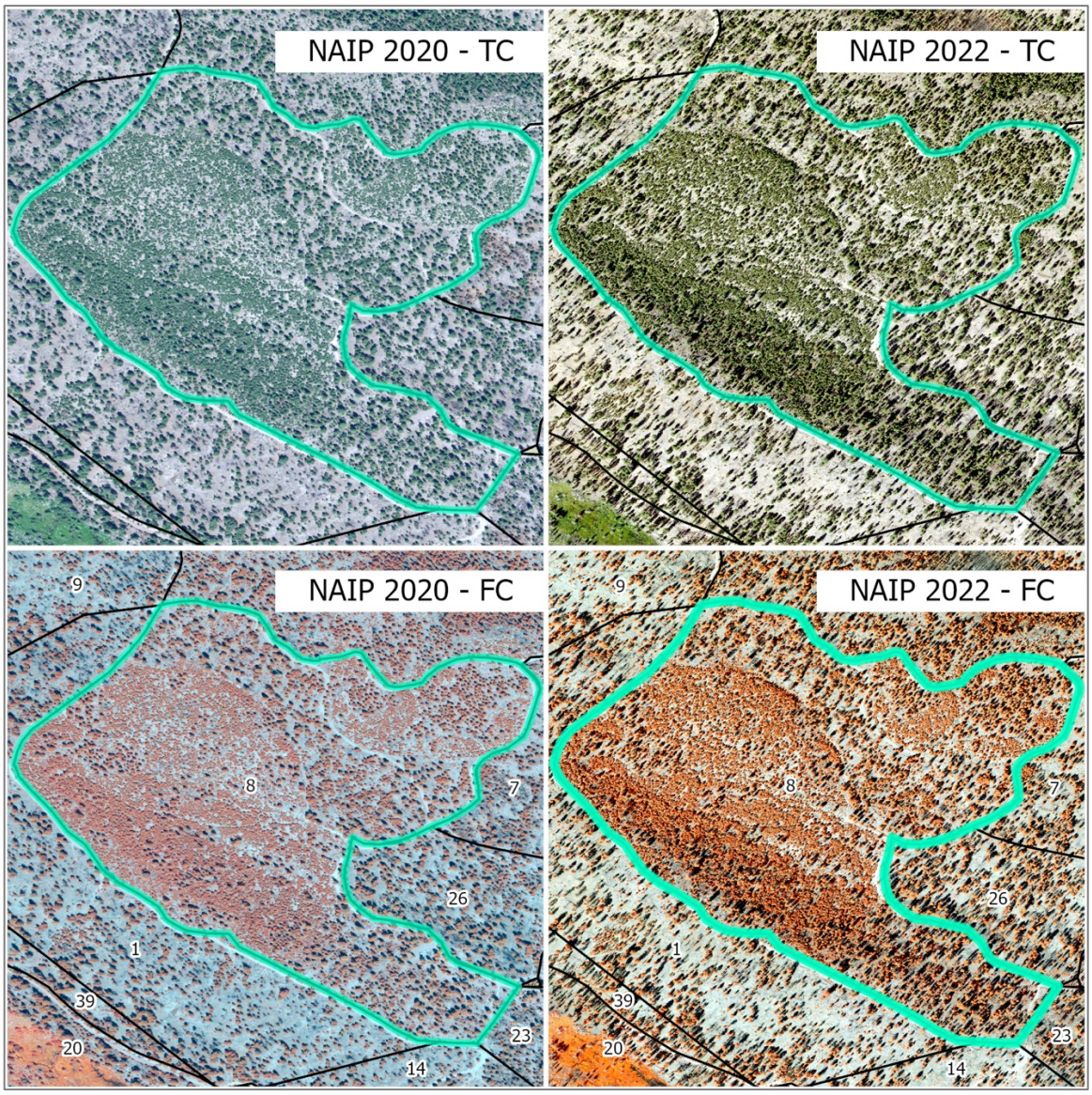

Fig. S1: Unit 8 (highlighted, see Fig. 1) as captured by NAIP 2020 in true color (TC), NAIP 2020 in false color (FS; NIR band in the red channel), NAIP 2022 in TC, and NAIP 2022 in FS. This figure shows how vegetation cover before the Rx treatment conducted in 2021 did not visibly change compared to vegetation cover after the 2021 Bootleg Fire (south-central Oregon, US). This indicates that both the Rx and the Bootleg Fire burned at very low severity in unit 8.

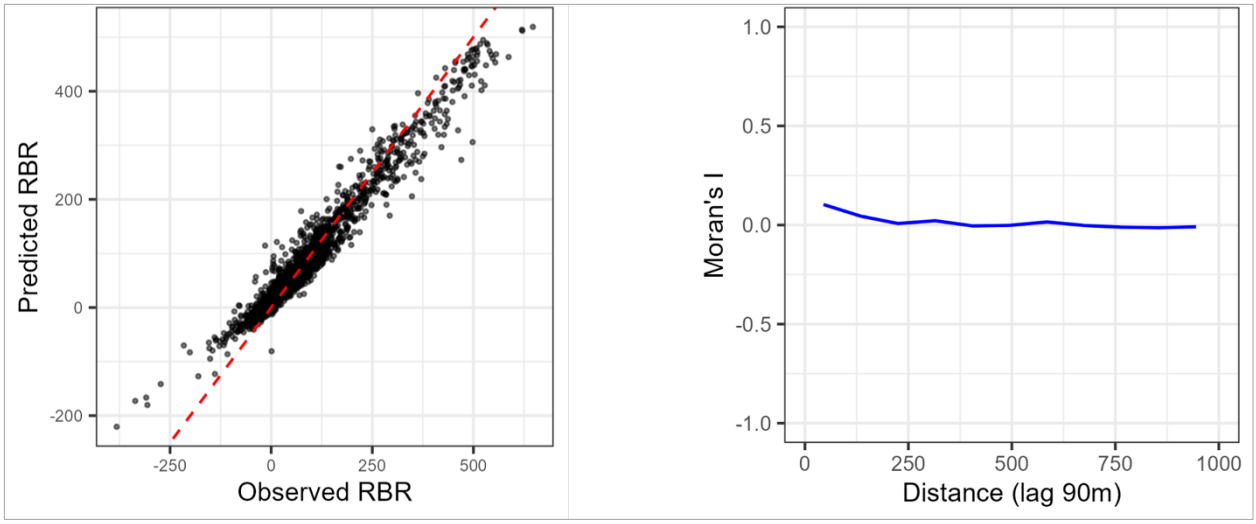

Fig. S2: Random Forests model performance represented by a scatterplot of observed vs. predicted RBR values against a 1:1 fit line (red dotted line) (left), and a Moran's I plot representing residuals' spatial autocorrelation (right).

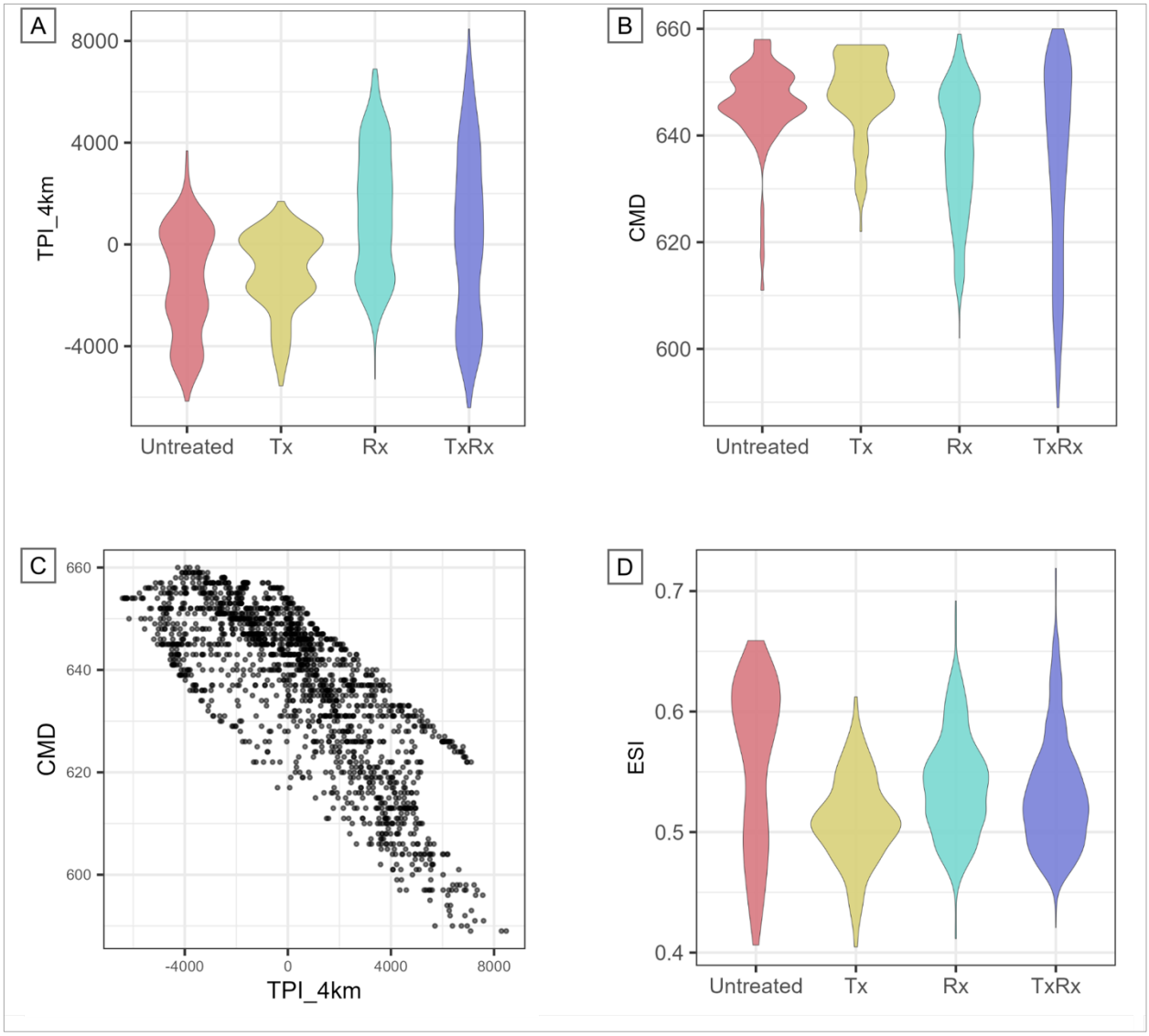

Fig. S3: A) TPI-4km distribution by treatment type; on the y-axis, negative values indicate flatter terrains and valleys, while positive values indicate hilltops and ridges. B) CMD distribution by treatment type; values on the y-axis indicate increasing moisture deficit. C) Relationship between CMD and TPI (bottom left; correlation = -0.8); scatterplot showing TPI-4km values on the x-axis and CMD values on the y-axis. D) ESI distribution by treatment type (bottom right); the y-axis indicates 0 for high water stress, and 1 for low water stress.

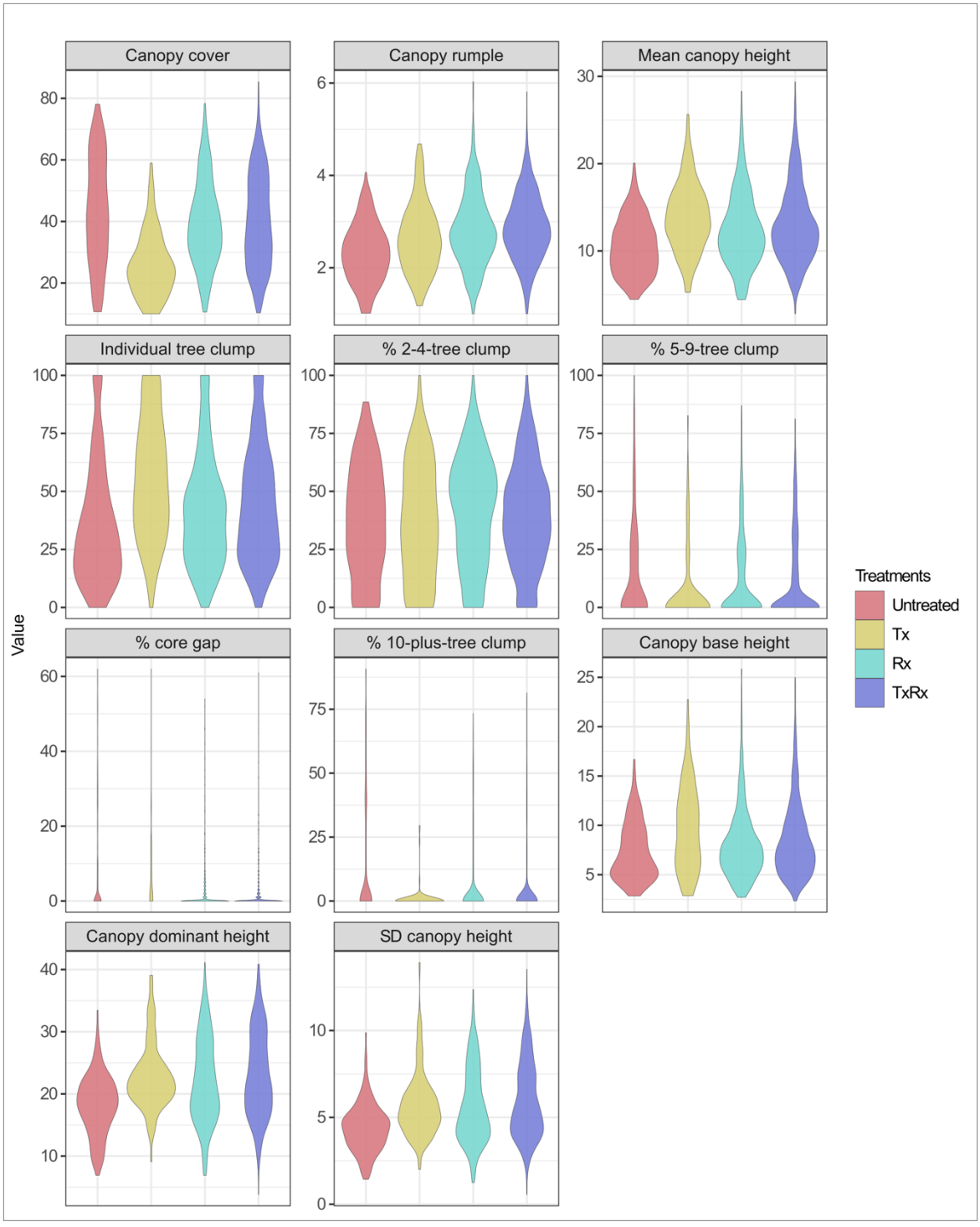

Fig. S4: Pre-Bootleg, LiDAR-derived forest metrics by treatment type. The dataset includes only observations with at least 10% canopy cover. LiDAR was collected in 2018.

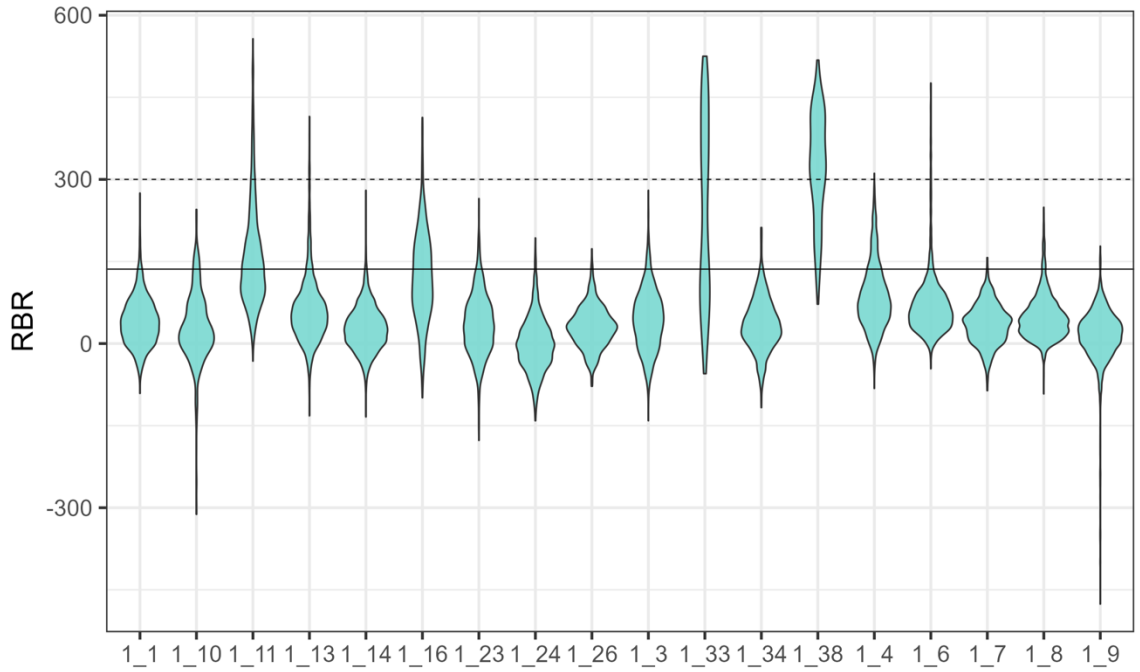

Fig. S5: Bootleg RBR distributions by individual units treated with Rx. Low and moderate burn severity thresholds are shown as solid and dotted black lines, respectively.

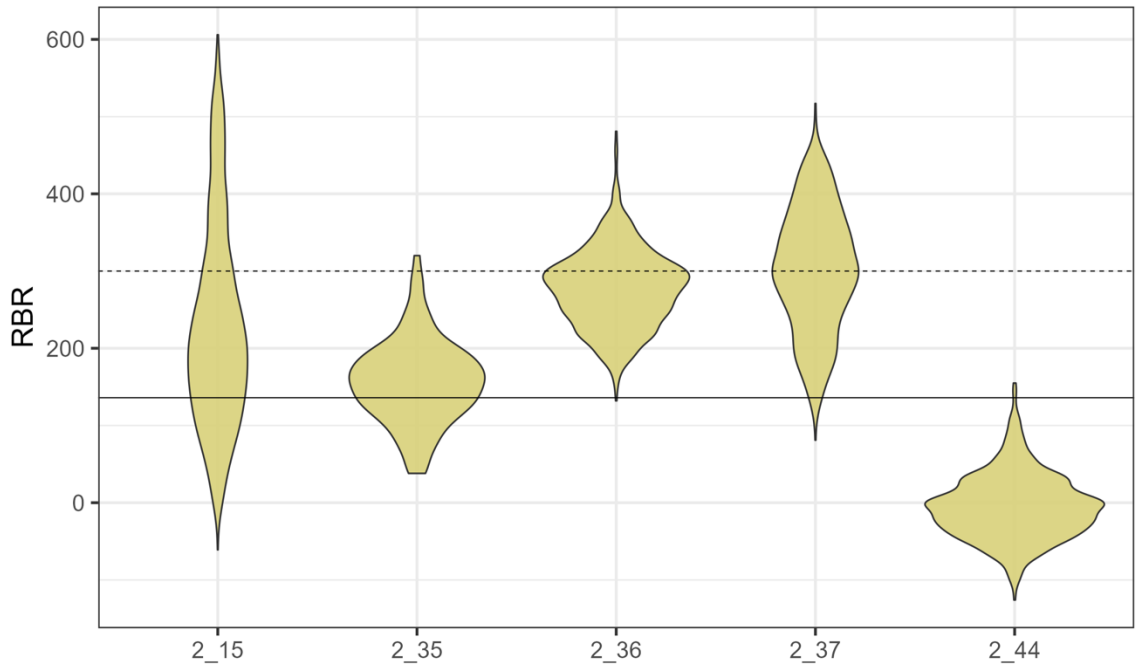

Fig. S6: Bootleg RBR distributions by individual units treated only with Tx. Low and moderate burn severity thresholds are shown as solid and dotted black lines, respectively.

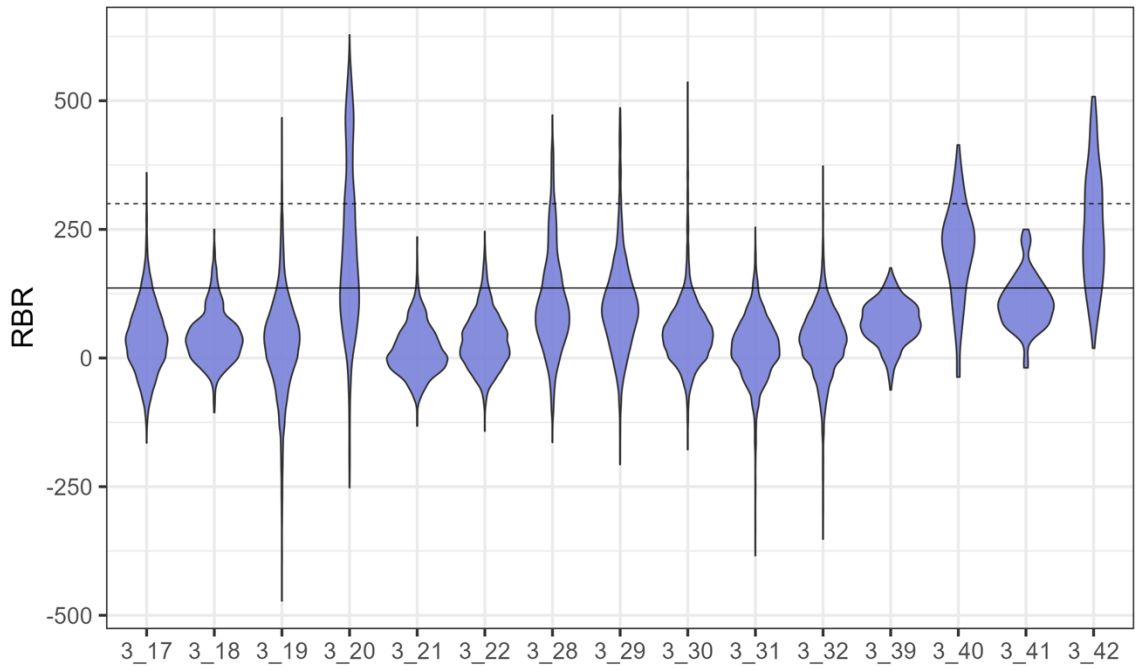

Fig. S7: Bootleg RBR distributions by individual units treated with TxRx. Low and moderate burn severity thresholds are shown as solid and dotted black lines, respectively.

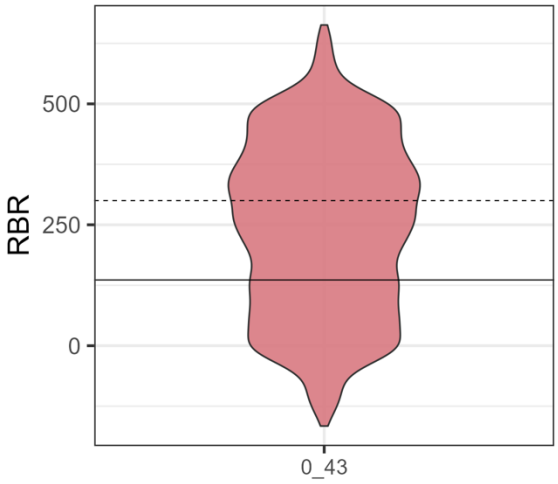

Fig. S8: Bootleg RBR distribution of untreated forest area. Low and moderate burn severity thresholds are shown as solid and dotted black lines, respectively.

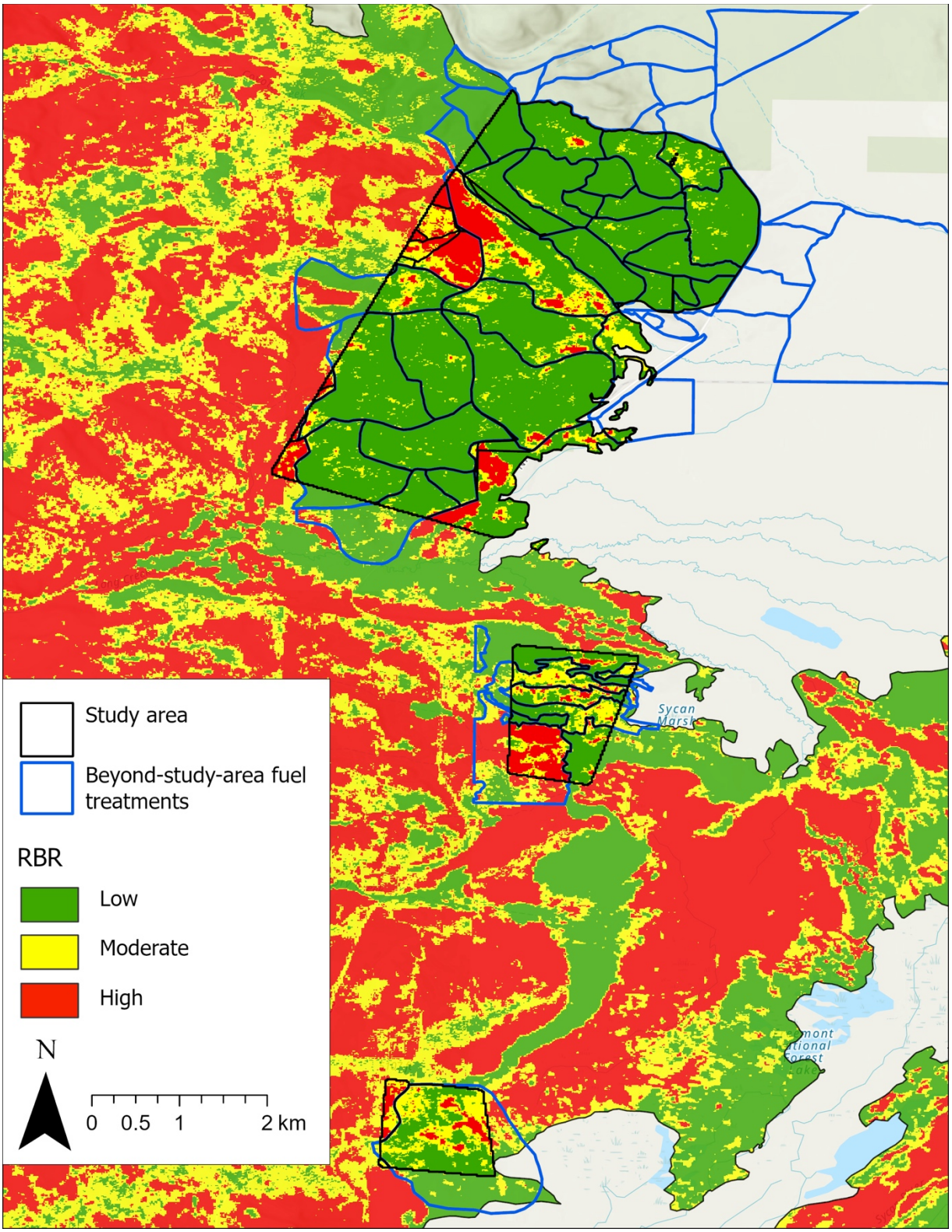

Fig. S9: Map of the 2021 Bootleg-Fire burn severity and fuel treatments conducted by TNC extending beyond our study area. Only treatments within our study area were considered in our analysis (see Fig. 1).